IFSM-79-95

INSTITUTE OF FRACTURE AND SOLID MECHANICS

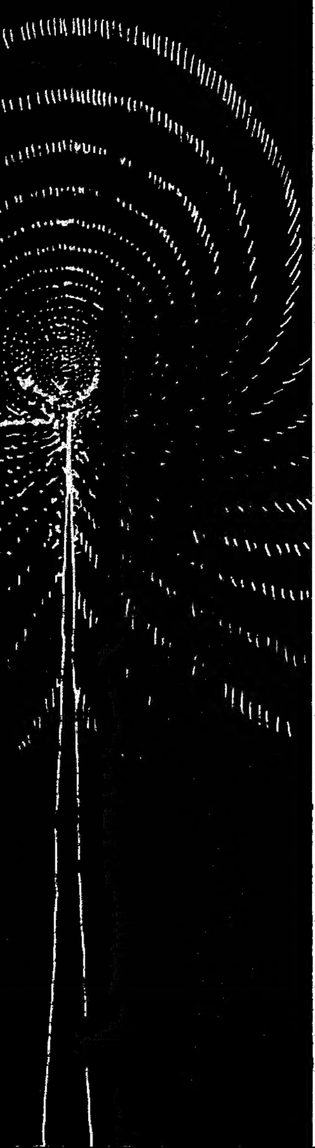

LEHIGH UNIVERSITY

HOMO MINISTER ET INTERPRES NATURAE • LEHIGH UNIVERSITY • FOUNDED BY ASA PACKER 1865

OFF-AXIS IMPACT OF UNIDIRECTIONAL COMPOSITES WITH CRACKS: DYNAMIC STRESS INTENSIFICATION

BY

G. C. SIH AND E. P. CHEN

JANUARY 1979

MATERIALS AND STRUCTURES DIVISION
NASA-LEWIS RESEARCH CENTER
CLEVELAND, OHIO 44135

1. Report No.	2. Government Accession No.	3. Recipient's Catalog No.
NASA CR 159537		

4. Title and Subtitle	5. Report Date
Off-Axis Impact of Unidirectional Composites With Cracks: Dynamic Stress Intensification	January 1979
	6. Performing Organization Code
7. Author(s) Dr. G. C. Sih and Dr. E. P. Chen	8. Performing Organization Report No.
	10. Work Unit No.
9. Performing Organization Name and Address Institute of Fracture and Solid Mechanics Lehigh University Bethlehem, PA 18015	11. Contract or Grant No. NSG 3179
	13. Type of Report and Period Covered Interim Report
12. Sponsoring Agency Name and Address National Aeronautics and Space Administration Washington DC 20546	14. Sponsoring Agency Code

15. Supplementary Notes
Project Manager, Dr. C. C. Chamis
Materials and Structures Division
NASA-Lewis Research Center
Cleveland, OH 44135

16. Abstract
The dynamic response of unidirectional composites under off-axis (angle loading) impact is analyzed by assuming that the composite contains an initial flaw in the matrix material. The analytical method utilizes Fourier transform for the space variable and Laplace transform for the time variable. The off-axis impact is separated into two parts; one being symmetric and the other skew-symmetric with reference to the crack plane. Transient boundary conditions of normal and shear tractions are applied to a crack embedded in the matrix of the unidirectional composite. The two boundard conditions are solved independently and the results superimposed. Mathematically, these conditions reduce the problem to a system of dual integral equations which are solved in the Laplace transform plane for the transform of the dynamic stress intensity factor. The time inversion is carried out numerically for various combinations of the material properties of the composite and the results are displayed graphically.

17. Key Words (Suggested by Author(s))	18. Distribution Statement
composites, off-axis impact, elastodynamics, stress analysis, through-cracks, stress intensity, Laplace transform, Fourier transform, Fredholm integral equations	Unclassified

19. Security Classif. (of this report)	20. Security Classif. (of this page)	21. No. of Pages	22. Price*
Unclassified	Unclassified	42	

* ~~For sale by the National Technical Information Service, Springfield, Virginia 22161~~

NASA-C-168 (Rev. 10-75)

FOREWORD

This research report is concerned with the dynamic response of unidirectional composites under off-axis impact and represents a portion of the work performed for the NASA-Lewis Research Center in Cleveland, Ohio for the period February 13, 1978 through February 12, 1979 under Grant NSG 3179 with the Institute of Fracture and Solid Mechanics at Lehigh University. The Principal Investigator of the project is Professor George C. Sih and the Associate Investigator is Dr. E. P. Chen who has since left Lehigh University and joined the Sandia Laboratory in New Mexico. The authors are grateful to the NASA Project Manager, Dr. Christos C. Chamis who has carefully reviewed this report and provided a number of concrete suggestions.

TABLE OF CONTENTS

LIST OF FIGURES

LIST OF SYMBOLS

a	- half of the crack length
$A(s,p), B(s,p)$	- unknowns in dual integral equations
$A^{(i)}, B^{(i)}, C^{(i)}$	- coefficients for transfer of solution, function of (s,p)
Br	- Bromwich contour in the complex p-plane
c_{1j}, c_{2j}	- dilatational and shear wave speeds for medium j
$f^*(p)$	- Laplace transform of f(t)
$f^c(s)$	- cosine transform of f(x)
$f^s(s)$	- sine transform of f(x)
$(f)_j$	- indicates that f is evaluated in medium j
$F_I(s,p), F_{II}(s,p)$	- kernels in dual integral equations
h	- half of the thickness of the layer
$H(t)$	- Heaviside unit step function
$J_o(x)$	- Bessel function of order 0
$k_1(t), k_2(t)$	- dynamic stress intensity factors
$K_I(\xi,\eta,p)$ $K_{II}(\xi,\eta,p)$	- kernels in Fredholm integral equations
$P_n(x)$	- Legendre polynomial
r_1, θ_1	- crack tip polar coordinates
t	- time
u_x, u_y	- displacement components
x, y, z	- rectangular coordinates - crack lies in the xz-plane
$\alpha^{(i)}$	- functions of (p,s) through γ_{ij}
$\beta^{(i)}, \Delta_o$	- functions of (p,s) through $\alpha^{(i)}$
γ_{ij}	- exponents for transform of solution, functions of (p,s)
δ	- step size for numerical inversion of Laplace transforms
Δ_I, Δ_{II}	- functions of (p,s) through $\beta^{(i)}$

κ_i	- parameters of dual integral equations
λ_1, λ_2	- Lamé coefficient
μ_1, μ_2	- shear modulus
ν_1, ν_2	- Poisson's ratio
ρ_1, ρ_2	- mass density
σ_o	- suddenly applied normal stress
$\sigma(t)$	- time-dependent remote applied stress
$\sigma_x, \sigma_y, \sigma_z, \tau_{xy}$	- stress components for plane strain
τ_o	- suddenly applied shear stress
ϕ_j, ψ_j	- scalar potentials for medium j
$\Phi^*_I(\xi,p), \Phi^*_{II}(\xi,p)$	- unknowns in Fredholm integral equations
∇^2	- Laplacian operator

OFF-AXIS IMPACT OF UNIDIRECTIONAL COMPOSITES WITH CRACKS:

DYNAMIC STRESS INTENSIFICATION

by

G. C. Sih
Institute of Fracture and Solid Mechanics
Lehigh University
Bethlehem, Pennsylvania 18015

and

E. P. Chen*
Sandia Laboratories
Albuquerque, New Mexico 87115

ABSTRACT

The dynamic response of unidirectional composites under off-axis (angle loading) impact is analyzed by assuming that the composite contains an initial flaw in the matrix material. Because of the complexities that arise from the interaction of waves scattered by the crack with those reflected by the interfaces within the composite, dynamic analyses of composites with cracks have been treated only for a few simple cases. One of the objectives of the present work is to develop an effective analytical method for determining dynamic stress solutions. This will not only lead to an in-depth understanding of the failure of composites due to impact but also provide reliable solutions that can guide the development of numerical methods.

The analysis method utilizes Fourier transform for the space variable and Laplace transform for the time variable. The time-dependent angle loading is

*This work was completed during Dr. Chen's tenure at Lehigh University.

separated into two parts: one being symmetric and the other skew-symmetric with reference to the crack plane. By means of superposition, the transient boundary conditions consist of applying normal and shear tractions to a crack embedded in the matrix of the unidirectional composite. Mathematically, these conditions reduce the problem to a system of dual integral equations which are solved in the Laplace transform plane for the transform of the dynamic stress intensity factor. The time inversion is carried out numerically for various combinations of the material properties of the composite and the results are displayed graphically.

INTRODUCTION

Past work on the development of high performance composite materials was mainly concerned with achieving high strength and modulus. This requirement alone, however, may result in a composite that is excessively brittle and lacks the ability to resist impact loading. The energy absorption or toughness of the composite is also an important property that must be accounted for in addition to strength and stiffness.

The concept of fracture toughness has mostly been applied to homogeneous isotropic materials [1] based on the linear fracture mechanics theories such as those advanced by Griffith, Irwin and others. These theories, developed for single-phase materials, have had limited success in characterizing the fracture behavior of composites which are inherently nonhomogeneous and anisotropic. This is mainly because the fracture modes in composites are multi-facet and can include interface failure, fiber breaking, matrix fracture, etc. The individual contribution of each of these failure modes is not clearly accounted for and/or not related to the critical failure load. As a result, large discrepancies

between the theory and experiment can result.

A study on the selection of appropriate mathematical models for different unidirectional composite systems was made [2] in the case of static loading. Many of the assumptions in [2] will also be used in the dynamic problem treated here. One of them is the existence of inherent flaws or cracks which are the sites of failure initiation.

Analytical investigation of the fracture of fibrous composite materials subjected to impact loading has been meager because the elastodynamic stress analysis involves numerous parameters and is enormously complex. This is necessitated by the complex nature of the dynamic load transfer characteristics in composites containing initial imperfections such as flaws or cracks. The stress wave solution is not only time-dependent but it interacts with the material properties of the constituents of the composite and the various geometric parameters. The influence of these parameters will be analyzed in this impact study with particular emphasis placed on determining the dynamic stress intensity factors k_1 and k_2 arising from normal and shear loading. Their combination (off-axis or angle loading) determines the response to loading of a more general nature and reflects the energy absorption property of the composite. Several examples of how k_1 and k_2 can be combined to predict crack behavior in dynamic stress fields are found in [3]. The question of whether there is the need of how to define a dynamic fracture toughness parameter differing from its corresponding static value has been the subject of many past and present debates within the fracture mechanics community. Thus far, no general agreement has been achieved.

This report is concerned with dynamic fracture analysis and, particularly, with the development of an analytical method for obtaining effective dynamic stress solutions to unidirectional composites with cracks embedded in the matrix. Other possible failure modes will be dealt with in future reports. Effective stress solutions for k_1 and k_2 are essential as they are the prerequisites for formulating failure criteria and guiding the development of numerical procedures.

ANGLE CRACK UNDER IMPACT

Figure 1(a) considers a crack in a layer of matrix material of thickness 2h. The composite is reinforced by unidirectional fibers that are aligned parallel with one another and make an angle with the time-dependent applied stress $\sigma(t)$. Without serious loss in generality, the composite is assumed to be modeled by a layer of cracked material with elastic properties μ_1, ν_1 and ρ_1 sandwiched in between two dissimilar media with properties μ_2, ν_2 and ρ_2, Figure 1(b). The number of layers surrounding the cracked layer is reasonably large so that the average shear modulus μ_2, Poisson's ratio ν_2 and mass density ρ_2 can be used.

The basic two-dimensional elastodynamic equations in the theory of elasticity can be expressed in terms of two scalar potentials $\phi_j(x,y,t)$ and $\psi_j(x,y,t)$ where i,j = 1,2 with 1 and 2 referring to the cracked layer and the surrounding material, respectively. In terms of the Lamé coefficients λ_j and μ_j, the dynamic stress components are

$$(\sigma_x)_j = \lambda_j \nabla^2 \phi_j + 2\mu_j \left(\frac{\partial^2 \phi_j}{\partial x^2} + \frac{\partial^2 \psi_j}{\partial x \partial y}\right)$$

$$(\sigma_y)_j = \lambda_j \nabla^2 \phi_j + 2\mu_j \left(\frac{\partial^2 \phi_j}{\partial y^2} - \frac{\partial^2 \psi_j}{\partial x \partial y}\right) \qquad (1)$$

$$(\sigma_z)_j = \frac{\lambda_j}{2} \left(\frac{\lambda_j + 2\mu_j}{\lambda_j + \mu_j}\right) \nabla^2 \phi_j$$

$$(\tau_{xy})_j = \mu_j \left(2 \frac{\partial^2 \phi_j}{\partial x \partial y} + \frac{\partial^2 \psi_j}{\partial y^2} - \frac{\partial^2 \psi_j}{\partial x^2}\right)$$

where $\nabla^2 = \partial^2/\partial x^2 + \partial^2/\partial y^2$ and the thickness shear stresses are assumed to vanish. The corresponding in-plane displacements are given by

$$(u_x)_j = \frac{\partial \phi_j}{\partial x} + \frac{\partial \psi_j}{\partial y}$$

$$(u_y)_j = \frac{\partial \phi_j}{\partial y} - \frac{\partial \psi_j}{\partial x} \qquad (2)$$

Under plane strain, the material elements are constrained in the z-direction. The governing differential equations can then be obtained from the equations of motion:

$$\nabla^2 \phi_j = \frac{1}{c_{1j}^2} \frac{\partial^2 \phi_j}{\partial t^2}$$

$$\nabla^2 \psi_j = \frac{1}{c_{2j}^2} \frac{\partial^2 \psi_j}{\partial t^2} \qquad (3)$$

in which c_{1j} and c_{2j} are the dilatational and shear wave velocities defined as

$$c_{1j} = \left(\frac{\lambda_j+2\mu_j}{\rho_j}\right)^{1/2}, \quad c_{2j} = \left(\frac{\mu_j}{\rho_j}\right)^{1/2} \tag{4}$$

The problem involves the determination of the potentials $\phi_j(x,y,t)$ and $\psi_j(x,y,t)$ in equations (3) from the transient boundary conditions of the crack problem.

The analysis may be simplified considerably if the problem is separated into two parts. The first concerns with normal stresses applied to the crack such that symmetry prevails about the x-axis in Figure 1(b) while the second deals with shear surface tractions so that the problem is skew-symmetric with reference to the x-axis. Both of these problems will be presented separately.

NORMAL IMPACT

Let the composite body be initially at rest such that the stresses are zero everywhere. Suddenly, at t=0, a normal stress of magnitude $-\sigma_0$ is applied to the top and bottom crack surfaces in Figure 1(b) and kept on the crack of length 2a thereafter. Referring to the set of axes x and y that are placed parallel and normal to the line crack, the following conditions are prescribed:

$$(\sigma_y)_1(x,o,t) = -\sigma_0 H(t); \; (\tau_{xy})_1(x,o,t) = 0, \; 0\leq x<a; \; t>0 \tag{5}$$

where H(t) is the Heaviside unit step function. The symmetry conditions about the axis y=0 are enforced by noting

$$(u_y)_1(x,o,t) = 0; \; (\tau_{xy})_1(x,o,t) = 0, \; x\geq a; \; t>0 \tag{6}$$

Perfect bonding will be assumed along the interfaces between material 1 and material 2. This requires the stresses and displacements to be continuous across $y = \pm h$. On account of symmetry, only the upper half plane $y \geq 0$ need to be considered, i.e.,

$$(\sigma_y)_1(x,h,t) = (\sigma_y)_2(x,h,t)$$

$$(\tau_{xy})_1(x,h,t) = (\tau_{xy})_2(x,h,t) \tag{7}$$

and for the stresses and

$$(u_x)_1(x,h,t) = (u_x)_2(x,h,t)$$

$$(u_y)_1(x,h,t) = (u_y)_2(x,h,t) \tag{8}$$

for the displacements.

Dual integral equations. It is convenient at this point to apply the Laplace transform to the time variable t which corresponds to p in the transformed plane. Consider the standard Laplace transform on f(t):

$$f^*(p) = \int_0^\infty f(t)\, e^{-pt} dt \tag{9}$$

whose inversion is

$$f(t) = \frac{1}{2\pi i} \int_{Br} f^*(p)\, e^{pt} dp \tag{10}$$

in which Br stands for the Bromwich path of integration. The application of equation (9) to equations (3) yields

$$\nabla^2\phi_j^* = \frac{p^2}{c_{1j}^2}\,\phi_j^*$$

$$\nabla^2\psi_j^* = \frac{p^2}{c_{2j}^2}\,\psi_j^* \tag{11}$$

Again, the condition of symmetry requires only the consideration of x and y in the first quadrant. The Fourier cosine and sine transforms defined by

$$f^c(s) = \int_0^\infty f(x)\,\cos(sx)dx$$

$$f(x) = \frac{2}{\pi}\int_0^\infty f^c(s)\,\cos(sx)ds \tag{12}$$

and

$$f^s(s) = \int_0^\infty f(x)\,\sin(sx)dx$$

$$f(x) = \frac{2}{\pi}\int_0^\infty f^s(s)\,\sin(sx)ds \tag{13}$$

are now applied to the space variable x. This simplifies equations (3) to a set of ordinary differential equations which can be solved giving

$$\phi_1^*(x,y,p) = \frac{2}{\pi}\int_0^\infty [A^{(1)}(s,p)e^{-\gamma_{11}y} + A^{(2)}(s,p)e^{\gamma_{11}y}]\,\cos(sx)ds$$

$$\psi_1^*(x,y,p) = \frac{2}{\pi}\int_0^\infty [B^{(1)}(s,p)e^{-\gamma_{21}y} + B^{(2)}(s,p)e^{\gamma_{21}y}] \sin(sx)ds \tag{14}$$

for the cracked matrix and

$$\phi_2^*(x,y,p) = \frac{2}{\pi}\int_0^\infty C^{(1)}(s,p)e^{-\gamma_{12}y} \cos(sx)ds$$

$$\tag{15}$$

$$\psi_2^*(s,y,p) = \frac{2}{\pi}\int_0^\infty C^{(2)}(s,p)e^{-\gamma_{22}y} \sin(sx)ds$$

for the averaged fiber-matrix material. In equations (14) and (15), the quantities γ_{1j} and γ_{2j} are given by

$$\gamma_{1j} = (s^2 + \frac{p^2}{c_{1j}^2})^{1/2}, \quad \gamma_{2j} = (s^2 + \frac{p^2}{c_{2j}^2})^{1/2} \tag{16}$$

The functions $A^{(1)}$, $A^{(2)}$, $B^{(1)}$,---, $C^{(2)}$ in equations (14) and (15) are determined from the transient boundary conditions. To this end, equations (5) and (6) will be written in the Laplace transform plane:

$$(\sigma_y^*)_1(x,o,p) = -\frac{\sigma_o}{p}; \quad (\tau_{xy}^*)_1(x,o,p) = 0, \quad 0\leq x<a \tag{17}$$

and

$$(u_y^*)_1(x,o,p) = 0; \quad (\tau_{xy}^*)_1(x,o,p) = 0, \quad x\geq a \tag{18}$$

In the same way, equations (7) become

$$(\sigma_y^*)_1(x,h,p) = (\sigma_y^*)_2(x,h,p)$$

$$(\tau_{xy}^*)_1(x,h,p) = (\tau_{xy}^*)_2(x,h,p) \tag{19}$$

and equations (8) take the forms

$$(u_x^*)_1(x,h,p) = (u_x^*)_2(x,h,p)$$

$$(u_y^*)_1(x,h,p) = (u_y^*)_2(x,h,p) \tag{20}$$

The stresses and displacements in equations (1) and (2) may also be transformed into the Laplace transform plane. Without going into details, the appropriate Laplace transform of the stress and displacement expressions in equations (17) to (20) may be used to satisfy all of the necessary boundary, symmetry and continuity conditions. This leads to the following set of dual integral equations:

$$\int_0^\infty A(s,p)\cos(sx)ds = 0, \quad x \geq a$$

$$\int_0^\infty sF_I(s,p)\, A(s,p)\cos(sx)ds = -\frac{\pi\sigma_0}{4\mu_1 p(1-\kappa_1^2)}, \quad x<a \tag{21}$$

in which $F_I(s,p)$ stands for the known function

$$F_I(s,p) = \frac{1}{s(1-\kappa_1^2)\Delta_I} \{[\frac{1}{4} (s^2+\gamma_{21}^2)^2 - s^2\gamma_{11}\gamma_{21}][\beta^{(2)} - \beta^{(3)}e^{-2(\gamma_{11}+\gamma_{21})h}]$$

$$+ s(s^2+\gamma_{21}^2)[\gamma_{21}(\beta^{(1)}\beta^{(4)} - \beta^{(2)}\beta^{(3)}) - \gamma_{11}]e^{-(\gamma_{11}+\gamma_{21})h}$$

$$+ [\frac{1}{4} (s^2+\gamma_{21}^2)^2 + s^2\gamma_{11}\gamma_{21}][\beta^{(4)}e^{-2\gamma_{21}h} - \beta^{(1)}e^{-2\gamma_{11}h}]\} \tag{22}$$

while the quantities κ_1 and Δ_I are defined as

$$\kappa_1 = (c_{21}/c_{11})^{1/2}$$

$$\Delta_I = \frac{p^2}{2c_{21}^2} \gamma_{11}[\beta^{(2)} + \beta^{(3)}\ e^{-2(\gamma_{11}+\gamma_{21})h} + \beta^{(4)}\ e^{-2\gamma_{21}h}$$

$$+ \beta^{(1)}\ e^{-2\gamma_{11}h}] \tag{23}$$

such that $\beta^{(1)}, \beta^{(2)}, ---, \beta^{(4)}$ are given by

$$\beta^{(1)} = (\alpha^{(3)}\alpha^{(6)} - \alpha^{(2)}\alpha^{(7)})/\Delta_o;\ \beta^{(2)} = (\alpha^{(4)}\alpha^{(6)} - \alpha^{(2)}\alpha^{(8)})/\Delta_o$$

$$\beta^{(3)} = (\alpha^{(1)}\alpha^{(7)} - \alpha^{(3)}\alpha^{(5)})/\Delta_o;\ \beta^{(4)} = (\alpha^{(1)}\alpha^{(8)} - \alpha^{(4)}\alpha^{(5)})/\Delta_o \tag{24}$$

where Δ_o is

$$\Delta_o = \alpha^{(1)}\alpha^{(6)} - \alpha^{(2)}\alpha^{(5)} \tag{25}$$

The quantities $\alpha^{(1)}, \alpha^{(2)}, ---, \alpha^{(8)}$ in equations (25) are complicated functions of s, p and the material constants. They are given by equations (I.1) in Appendix I.

The problem is now reduced to finding the single unknown $A(s,p)$ governed by equations (21). Once $A(s,p)$ is known, the functions $A^{(1)}$, $A^{(2)}$,---, $C^{(2)}$ that are required in equations (14) and (15) for the Laplace transform of the potentials $\phi_j^*(x,y,p)$ and $\psi_j^*(x,y,p)$ can be obtained from equations (I.2) outlined in Appendix I. What remains is the determination of a solution for the dual integral equations (21). This will be accomplished with the help of a method by Copson [5] which has been used by Chen and Sih [6] for solving dynamic crack problems involving single-phase homogeneous materials. Following the details in [5,6], it can be shown that

$$A(s,p) = -\frac{\pi\sigma_0 a^2}{4\mu_1 p(1-\kappa_1^2)} \int_0^1 \sqrt{\xi}\ \Phi_I^*(\xi,p)\ J_0(sa\xi)d\xi \tag{26}$$

is a solution of equations (21) with J_0 being the zero order Bessel function of the first kind. The function $\Phi_I^*(\xi,p)$ is calculated numerically from a Fredholm integral equation of the second kind:

$$\Phi_I^*(\xi,p) + \int_0^1 \Phi_I^*(\eta,p)\ K_I(\xi,\eta,p)d\eta = \sqrt{\xi} \tag{27}$$

whose kernel

$$K_I(\xi,\eta,p) = \sqrt{\xi\eta} \int_0^\infty s[F_I(\tfrac{s}{a}, p) - 1]\ J_0(s\xi)\ J_0(s\eta)ds \tag{28}$$

is symmetric in ξ and η.

Mode I dynamic stress intensity factor. The transmission of the time-dependent load to the vicinity of the crack tip can be best described by the intensification of the local stresses. A quantity that has been used widely in

the static theory of fracture mechanics is the "stress intensity factor" which can be extracted from the asymptotic expansions of the stresses near the crack tip. Referring to Figure 2, let r_1 and θ_1 be a set of local polar coordinates measured from the right hand crack tip located at x=a and y=0 in the matrix material, the singular character of the dynamic stresses is described only by the space variables and hence can be more easily determined in the Laplace transform domain. This observation was first made by Sih, Ravera and Embley [7]. Following their procedure, the local stresses in terms of r_1 and θ_1 are found:

$$(\sigma_x^*)_1(r_1,\theta_1,p) = \frac{k_1^*(p)}{\sqrt{2r_1}} \cos\frac{\theta_1}{2}\left(1 - \sin\frac{\theta_1}{2}\sin\frac{3\theta_1}{2}\right) + 0(r_1^\circ)$$

$$(\sigma_y^*)_1(r_1,\theta_1,p) = \frac{k_1^*(p)}{\sqrt{2r_1}} \cos\frac{\theta_1}{2}\left(1 + \sin\frac{\theta_1}{2}\sin\frac{3\theta_1}{2}\right) + 0(r_1^\circ)$$

$$(\sigma_z^*)_1(r_1,\theta_1,p) = \frac{k_1^*(p)}{\sqrt{2r_1}} 2\nu_1 \cos\frac{\theta_1}{2} + 0(r_1^\circ) \tag{29}$$

$$(\tau_{xy}^*)_1(r_1,\theta_1,p) = \frac{k_1^*(p)}{\sqrt{2r_1}} \sin\frac{\theta_1}{2}\cos\frac{\theta_1}{2}\cos\frac{3\theta_1}{2} + 0(r_1^\circ)$$

Only the dynamic stress intensity factor, $k_1^*(p)$, in equations (29) need to be inverted to real time t:

$$k_1^*(p) = \frac{\Phi_I^*(1,p)}{p}\sigma_o\sqrt{a} \tag{30}$$

where the function $\Phi_I^*(1,p)$ is found from $\Phi_I^*(\xi,p)$ by letting the nondimensional parameter ξ=1 representing the crack tip location. The functional dependence

of the stresses in r_1 and θ_1 as shown by equations (29) reveals that the dynamic stresses also possess the inverse square root singularity in terms of r_1 and that the angular distribution in θ, is the same as the case for static loading.

Applying the Laplace inversion formula in equation (10) to (30) renders the factor $k_1(t)$ as a function of time, i.e.,

$$k_1(t) = \frac{\sigma_0\sqrt{a}}{2\pi i}\int_{Br} \frac{\Phi_I^*(1,p)}{p} e^{pt}dp \qquad (31)$$

It is apparent that $\Phi_I^*(1,p)$ must be first known before the integration of equation (31) can be performed. Refer to Appendix II for a detailed account of the procedure used for evaluating equation (31). Three different sets of $\Phi_I^*(1,p)$ values are plotted against the dimensionless Laplace transform wave number c_{21}/pa. They are given in Figures 3 to 5 for $\rho_1 = \rho_2$ and $\nu_1 = \nu_2 = 0.29$ while the ratios a/h and μ_2/μ_1 are varied. In general, all the curves tend to rise quickly and then flatten out. It would be more meaningful to discuss the influence of a/h and μ_2/μ_1 on the stress intensity factor $k_1(t)$.

Figures 6 to 8 display the normalized stress intensity factor $k_1(t)/\sigma_0\sqrt{a}$ as a function of $c_{21}t/a$. In Figure 6, the crack length to layer thickness ratio, a/h, is fixed at unity while the shear moduli ratio, μ_2/μ_1 is increased from 0.1 to 10.0 as indicated. The $k_1(t)$ factor is oscillatory in nature reaching a peak and then decreases in magnitude as time increases. The oscillation is more pronounced when the shear modulus of the cracked material is greater than that of the surrounding material, i.e., $\mu_1 > \mu_2$. The values of $k_1(t)$ decrease below those of the corresponding homogeneous case, $\mu_1 = \mu_2$, solved previously by Chen and Sih [6] when $\mu_1 < \mu_2$. The influence of a/h on $k_1(t)$ is exhibited in Figures 7 and 8 for the two cases of $\mu_2/\mu_1 = 0.1$ and 10.0, respectively. For $\mu_2/\mu_1 = 0.1$

in Figure 7, a decrease in a/h tends to lower the stress intensity factor. Observed also is a small step in the curve for a/h = 2.0 and small time t. This corresponds to the reflection of elastic waves from the material interface. The size and time scale are such that this effect showed up quantitatively in the graph while the same effect was not noticeable in the other curves. For the smaller ratios of a/h such as 0.5 and 1.0, the crack tips are further away from the interface and the influence of the reflected waves are not as pronounced. The opposite trend is observed in Figure 8 for $\mu_2/\mu_1 = 10.0$. When the outer material is more rigid than that of the center layer, $k_1(t)$ tends to increase in magnitude as a/h is decreased. Again, a distinct step in the curve for a/h = 2.0 is seen for small time t. As time increases, all of the results here reduce to the corresponding static solutions of Hilton and Sih [8].

General loading. If the normal stress applied to the crack surface is not constant in magnitude but may vary as a function of x, then the dynamic stress intensity factor can be obtained by adding a sequence of solutions corresponding to step loadings with different stress levels σ_0, σ_1, etc. In other words, the general loading $\sigma(t)$ may be considered as the sum:

$$\sigma(t) = \sigma_0 H(t_0) + \sigma_1 H(t_1) + \sigma_2 H(t_2) + \ldots \tag{32}$$

This is illustrated graphically in Figure 9. From equations (31) and (32), the factor $k_1(t)$ that corresponds to $\sigma(t)$ may be written down immediately as follows:

$$k_1(t) = \frac{1}{2\pi i}\left[\sigma_0 H(t_0) + \sigma_1 H(t_1) + \ldots\right] \int_{Br} \frac{\Phi_I^*(1,p)}{p} e^{pt} dp \tag{33}$$

Equation (33) may be used to derive $k_1(t)$ for any time-dependent normal surface tractions which in turn can also simulate any loadings that are applied at dis-

tances away from the crack by means of the principle of superposition.

SHEAR IMPACT

Suppose that the crack in Figure 1(b) is now sheared suddenly by a pair of shear stresses of magnitude $-\tau_0$ such that the upper and lower crack surfaces move in the opposite direction. This creates a deformation field that is skew-symmetric with respect to the y=0 plane. Following the footstep laid out in the previous example on normal impact, the Laplace transform of the transient boundary conditions on the x-axis inside the crack are

$$(\tau^*_{xy})_1(x,o,p) = -\frac{\tau_0}{p};\ (\sigma^*_y)_1(x,o,p) = 0,\ 0\leq x<a \tag{34}$$

and the skew-symmetric conditions outside the crack are given by

$$(u^*_x)_1(x,o,p) = 0;\ (\sigma^*_y)_1(x,o,p) = 0,\ x\geq a \tag{35}$$

Continuity of the stresses across y=h is expressed by

$$\begin{aligned}(\sigma^*_y)_1(x,h,p) &= (\sigma^*_y)_2(x,h,p)\\ (\tau^*_{xy})_1(x,h,p) &= (\tau^*_{xy})_2(x,h,p)\end{aligned} \tag{36}$$

while the displacements are also required to be continuous, i.e.,

$$\begin{aligned}(u^*_x)_1(x,h,p) &= (u^*_x)_2(x,h,p)\\ (u^*_y)_1(x,h,p) &= (u^*_y)_2(x,h,p)\end{aligned} \tag{37}$$

Integral representations. Under the above considerations, the following wave potentials $\phi_j^*(x,y,p)$ and $\psi_j^*(x,y,p)$ are selected:

$$\phi_1^*(x,y,p) = \frac{2}{\pi}\int_0^\infty [A^{(1)}(s,p)e^{-\gamma_{11}y} + A^{(2)}(s,p)e^{\gamma_{11}y}] \sin(sx)ds$$

$$\psi_1^*(x,y,p) = \frac{2}{\pi}\int_0^\infty [B^{(1)}(s,p)e^{-\gamma_{21}y} + B^{(2)}(s,p)e^{\gamma_{21}y}] \cos(sx)ds \tag{38}$$

for the cracked layer and

$$\phi_2^*(x,y,p) = \frac{2}{\pi}\int_0^\infty C^{(1)}(s,p)e^{-\gamma_{12}y} \sin(sx)ds$$

$$\psi_2^*(x,y,p) = \frac{2}{\pi}\int_0^\infty C^{(2)}(s,p)e^{-\gamma_{22}y} \cos(sx)ds \tag{39}$$

for the outside material.

Equations (38) and (39) may now be substituted into the Laplace transform of the stresses and displacements in equations (1) and (2). Making use of the conditions in equations (34) to (37), the solution can be expressed in terms of the functions $A^{(1)}$, $A^{(2)}$,---, $C^{(2)}$ which are related to a single unknown $B(s,p)$ as shown by equations (III.1) in Appendix III. The function $B(s,p)$ is governed by the system of dual integral equations

$$\int_0^\infty B(s,p) \cos(sx)ds = 0, \quad x \geq a$$

$$\int_0^\infty sF_{II}(s,p)\, B(s,p) \cos(sx)ds = \frac{\pi\tau_0}{4\mu_1 p(1-\kappa_1^2)}, \quad x<a \tag{40}$$

The function $F_{II}(s,p)$ is related to $F_I(s,p)$ in equation (22) as

$$F_{II}(s,p) = \frac{\Delta_I}{\Delta_{II}} F_I(s,p) \tag{41}$$

where

$$\Delta_{II} = \frac{p^2}{2c_{21}^2} \gamma_{21}[\beta^{(2)} + \beta^{(3)} e^{-2(\gamma_{11}+\gamma_{21})h} - \beta^{(4)} e^{-2\gamma_{21}h} - \beta^{(1)} e^{-2\gamma_{11}h}] \tag{42}$$

The other parameters such as κ_1, Δ_I, $\beta^{(1)}$, $\beta^{(2)}$, etc., are the same as those defined earlier for the case of normal impact.

A solution to equations (40) is again found by application of the Copson's method [5]:

$$B(s,p) = \frac{\pi\tau_o a^2}{4\mu_1 p(1-\kappa_1^2)} \int_0^1 \sqrt{\xi}\ \Phi_{II}^*(\xi,p)\ J_o(sa\xi)d\xi \tag{43}$$

provided that $\Phi_{II}^*(\xi,p)$ satisfies a Fredholm integral equation of the second kind:

$$\Phi_{II}^*(\xi,p) + \int_0^1 \Phi_{II}^*(\eta,p)\ K_{II}(\xi,\eta,p)d\eta = \sqrt{\xi} \tag{44}$$

whose kernel $K_{II}(\xi,\eta,p)$ takes the form

$$K_{II}(\xi,\eta,p) = \sqrt{\xi\eta} \int_0^\infty s[F_{II}(\frac{s}{a}, p) - 1]\ J_o(s\xi)\ J_o(s\eta)ds \tag{45}$$

Mode II dynamic stress intensity factor. As in the case of Mode I, the asymptotic expressions of the dynamic stresses in the Laplace transform plane are first obtained in terms of r_1 and θ_1 defined in Figure 2. The results are

$$(\sigma_x^*)_1(r_1,\theta_1,p) = -\frac{k_2^*(p)}{\sqrt{2r_1}} \sin\frac{\theta_1}{2}\left(2 + \cos\frac{\theta_1}{2}\cos\frac{3\theta_1}{2}\right) + O(r_1^\circ)$$

$$(\sigma_y^*)_1(r_1,\theta_1,p) = \frac{k_2^*(p)}{\sqrt{2r_1}} \sin\frac{\theta_1}{2}\cos\frac{\theta_1}{2}\cos\frac{3\theta_1}{2} + O(r_1^\circ)$$

$$(\sigma_z^*)_1(r_1,\theta_1,p) = -\frac{k_2^*(p)}{\sqrt{2r_1}} 2\nu_1 \sin\frac{\theta_1}{2} + O(r_1^\circ) \tag{46}$$

$$(\tau_{xy}^*)_1(r_1,\theta_1,p) = \frac{k_2^*(p)}{\sqrt{2r_1}} \sin\frac{\theta_1}{2}\cos\frac{\theta_1}{2}\cos\frac{3\theta_1}{2} + O(r_1^\circ)$$

with $k_2^*(p)$ being the only quantity that depends on time through the parameter p:

$$k_2^*(p) = \frac{\Phi_{II}^*(1,p)}{p}\tau_o\sqrt{a} \tag{47}$$

Equation (10) is then applied to invert the Laplace transform of the stress intensity factor in equation (47). This gives

$$k_2(t) = \frac{\tau_o\sqrt{a}}{2\pi i}\int_{Br}\frac{\Phi_{II}^*(1,p)}{p}e^{pt}dp \tag{48}$$

in which $\Phi_{II}^*(1,p)$ is computed numerically from equation (44).

Figures 10 to 12 display the values of $\Phi_{II}^*(1,p)$ as a function of the normalized quantity c_{21}/pa for various values of a/h and μ_2/μ_1 while $\nu_1 = \nu_2 = 0.29$ and $\rho_1 = \rho_2$ are used for all cases. With a knowledge of $\Phi_{II}^*(1,p)$, the integral in equation (48) may be evaluated by a procedure outlined in Appendix II. In general, $k_2(t)$ increases with time reaching a maximum and then decreases to the static value for sufficiently large time. The trend is very similar to $k_1(t)$

for the case of normal impact in that a higher value of $k_2(t)$ is obtained when the modulus of the surrounding material is less than that of the cracked layer, i.e., $\mu_2/\mu_1 < 1$. Comparing the results in Figures 6 and 12, it is seen that for $\mu_2/\mu_1 < 1$, normal impact yields a higher crack tip stress intensity factor than shear impact, i.e., $k_1(t) > k_2(t)$. The opposite is observed when $\mu_2/\mu_1 > 1$, i.e., $k_2(t) > k_1(t)$. The curves in Figures 14 and 15 for $k_2(t)$ also show the absence of a small fluctuation for small time which was present in Figures 7 and 8 for $k_1(t)$. This is because the influence of the reflected incident shear wave from the interface is considerably weaker even for the ratio of $a/h = 2.0$.

CONCLUSION

As composite materials are currently being applied to major primary structure designs, it is necessary to have an in-depth understanding of the mechanical behavior of these materials, particularly with reference to the allowable applied load both statically and dynamically. This investigation is concerned with the dynamic stress distribution around a crack embedded in the matrix of a unidirectional composite. The time-dependent loading can be of a general nature applied in an arbitrarily direction with reference to the crack plane. For those composites which fail predominantly by matrix cracking under impact, the present results can be used effectively for determining the ability of the composite to absorb energy and to withstand load prior to total destruction.

The other modes of failure such as fiber breaking and/or debonding of fibers from matrix are not treated but may be significant in other composite systems. The redistribution of dynamic stresses in these cases may also be analyzed such that their individual contribution can be assessed quantitatively. These cases will be left for future investigations.

APPENDIX I: EXPRESSIONS FOR $\alpha^{(i)}$ AND $A^{(i)}(s,p)$,---, $C^{(i)}(s,p)$ IN NORMAL LOADING

This section gives the expressions for $\alpha^{(1)}$, $\alpha^{(2)}$,---, $\alpha^{(8)}$ in equations (25) in terms of the variables s, p and the material constants

$$\alpha^{(1)} = -s[(1-\frac{\mu_2}{\mu_1})\gamma_{21} - \frac{\mu_2}{\mu_1}(\frac{p^2}{2c_{22}^2})(\frac{\gamma_{21}-\gamma_{22}}{s^2-\gamma_{12}\gamma_{22}})]$$

$$\alpha^{(2)} = s[(1-\frac{\mu_2}{\mu_1})\gamma_{21} - \frac{\mu_2}{\mu_1}(\frac{p^2}{2c_{22}^2})(\frac{\gamma_{21}+\gamma_{22}}{s^2-\gamma_{12}\gamma_{22}})]$$

$$\alpha^{(3)} = \frac{1}{2}(s^2+\gamma_{21}^2) - \frac{\mu_2}{\mu_1}[s^2 + \frac{p^2}{2c_{22}^2}(\frac{s^2-\gamma_{11}\gamma_{22}}{s^2-\gamma_{12}\gamma_{22}})]$$

$$\alpha^{(4)} = \frac{1}{2}(s^2+\gamma_{21}^2) - \frac{\mu_2}{\mu_1}[s^2 + \frac{p^2}{2c_{22}^2}(\frac{s^2+\gamma_{11}\gamma_{22}}{s^2-\gamma_{12}\gamma_{22}})]$$

$$\alpha^{(5)} = -\frac{1}{2}(s^2+\gamma_{21}^2) + \frac{\mu_2}{\mu_1}[s^2 + \frac{p^2}{2c_{22}^2}(\frac{s^2-\gamma_{12}\gamma_{21}}{s^2-\gamma_{12}\gamma_{22}})] \qquad (I.1)$$

$$\alpha^{(6)} = -\frac{1}{2}(s^2+\gamma_{21}^2) + \frac{\mu_2}{\mu_1}[s^2 + \frac{p^2}{2c_{22}^2}(\frac{s^2+\gamma_{12}\gamma_{21}}{s^2-\gamma_{12}\gamma_{22}})]$$

$$\alpha^{(7)} = s[(1-\frac{\mu_2}{\mu_1})\gamma_{11} - \frac{\mu_2}{\mu_1}(\frac{p^2}{2c_{22}^2})(\frac{\gamma_{11}-\gamma_{12}}{s^2-\gamma_{12}\gamma_{22}})]$$

$$\alpha^{(8)} = -s[(1-\frac{\mu_2}{\mu_1})\gamma_{11} - \frac{\mu_2}{\mu_1}(\frac{p^2}{2c_{22}^2})(\frac{\gamma_{11}+\gamma_{12}}{s^2-\gamma_{12}\gamma_{22}})]$$

in which γ_{ij} is given by equations (16).

The functions $A^{(1)}$, $A^{(2)}$,---, $C^{(2)}$ are related to the single function $A(s,p)$ as follows:

$$A^{(1)}(s,p) = \frac{A(s,p)}{\Delta_I} [\frac{1}{2} (s^2+\gamma_{21}^2)(\beta^{(2)} + \beta^{(4)} e^{-2\gamma_{21}h}) - s\gamma_{11} e^{-(\gamma_{11}+\gamma_{21})h}]$$

$$A^{(2)}(s,p) = - \frac{A(s,p)}{\Delta_I} [s\gamma_{11} e^{-(\gamma_{11}+\gamma_{21})h} + \frac{1}{2} (s^2+\gamma_{21}^2) e^{-2\gamma_{11}h} (\beta^{(1)} + \beta^{(3)} e^{-2\gamma_{21}h})]$$

$$B^{(1)}(s,p) = \beta^{(1)} e^{-(\gamma_{11}-\gamma_{21})h} A^{(1)}(s,p) + \beta^{(2)} e^{(\gamma_{11}+\gamma_{21})h} A^{(2)}(s,p)$$

$$B^{(2)}(s,p) = \beta^{(3)} e^{-(\gamma_{11}+\gamma_{21})h} A^{(1)}(s,p) + \beta^{(4)} e^{(\gamma_{11}-\gamma_{21})h} A^{(2)}(s,p)$$

$$\begin{aligned} C^{(1)}(s,p) = \frac{e^{\gamma_{12}h}}{s^2-\gamma_{12}\gamma_{22}} [&(s^2-\gamma_{11}\gamma_{22}) e^{-\gamma_{11}h} A^{(1)}(s,p) \\ &+ (s^2+\gamma_{11}\gamma_{22}) e^{\gamma_{11}h} A^{(2)}(s,p) + s(\gamma_{21}-\gamma_{22}) e^{-\gamma_{21}h} B^{(1)}(s,p) \\ &- s(\gamma_{21}+\gamma_{22}) e^{\gamma_{21}h} B^{(2)}(s,p)] \end{aligned} \qquad (I.2)$$

$$\begin{aligned} C^{(2)}(s,p) = \frac{e^{\gamma_{22}h}}{s^2-\gamma_{12}\gamma_{22}} [&s(\gamma_{11}-\gamma_{12}) e^{-\gamma_{11}h} A^{(1)}(s,p) \\ &- s(\gamma_{11}+\gamma_{22}) e^{\gamma_{11}h} A^{(2)}(s,p) + (s^2-\gamma_{12}\gamma_{21}) e^{-\gamma_{21}h} B^{(1)}(s,p) \\ &+ (s^2+\gamma_{12}\gamma_{21}) e^{\gamma_{21}h} B^{(2)}(s,p)] \end{aligned}$$

APPENDIX II: METHOD FOR EVALUATING THE DYNAMIC STRESS INTENSITY FACTOR EQUATION (31)

The integral in equation (31) is basically of the form

$$g(t) = \frac{1}{2\pi i} \int_{Br} \frac{f^*(1,p)}{p} e^{pt} dp \tag{II.1}$$

The Bromwich path, Br, consists of an infinite line parallel to and to the right of the imaginary axis in the complex p-plane. The function* $f^*(1,p)$ is considered to be known for discrete values of p. There are a number of available methods for finding g(t) as a process in the Laplace inverse transform. The method adopted here can be found in [9,10].

The integral $f^*(1,p)/p$ in equation (II.1) is first evaluated at the points

$$p = (1+n)\delta, \quad n = 0,1,2,--- \tag{II.2}$$

in which δ is a real and positive number. According to equations (9) and (10), $f^*(1,p)/p$ may be written as

$$\frac{f^*(1,p)}{p} = \int_0^\infty g(t)e^{-pt}dt \tag{II.3}$$

The above infinite integral is now transformed to a finite integral on the interval [-1,1] by making the substitutions

---

*$f^*(1,p)$ stands for $\Phi^*_{I}(1,p)$ in normal impact and $\Phi^*_{II}(1,p)$ in shear impact and they are calculated from the Fredholm integral equations of the second kind, namely equations (27) and (44).

$$x = 2e^{-\delta t} - 1 \tag{II.4}$$

and

$$G(x) = g[t(x)] = g[-\frac{1}{\delta}\log(\frac{x+1}{2})] \tag{II.5}$$

Therefore, equation (II.3) becomes

$$\frac{f^*[1,(1+n)\delta]}{1+n} = \frac{1}{2^{n+1}}\int_{-1}^{1} (1+x)^n\, G(x)dx \tag{II.6}$$

in which $G(x)$ can be expanded in series form consisting of Legendre polynomials $P_n(x)$ which are orthogonal on the interval [-1,1], i.e.,

$$G(x) = \sum_{i=0}^{\infty} C_i\, P_i(x) \tag{II.7}$$

Similarly, the function $(1+x)^n$ in equation (II.6) may also be expanded in the form

$$(1+x)^n = \sum_{i=0}^{n} D_i\, P_i(x) \tag{II.8}$$

such that

$$D_i = 2^n(2i+1)\,\frac{n(n-1)---[n-(i-1)]}{(n+1)(n+2)---(n+i+1)} \tag{II.9}$$

Putting equations (II.7) and (II.8) into (II.6) and applying the orthogonality conditions for the Legendre polynomials, the following sum is established:

$$\frac{f^*[1,(1+n)\delta]}{1+n} = \sum_{i=0}^{n} \frac{n(n-1)---[n-(i-1)]}{(n+1)(n+2)---(n+i+1)} C_i \tag{II.10}$$

Thus the coefficients C_i may be found with C_0 given by

$$C_0 = f^*(1,\delta) \tag{II.11}$$

For a finite number of N coefficients, a partial sum for G(x) in (II.7) is obtained and an approximate evaluation of g(t) can be made since from equation (II.5)

$$g(t) = \sum_{i=0}^{N-1} C_i P_i \; [2e^{-\delta t} - 1] \tag{II.12}$$

The parameter δ is chosen such that g(t) is best described for the range of t considered.

APPENDIX III: EXPRESSIONS FOR $A^{(i)}(s,p)$,---, $C^{(i)}(s,p)$ IN SHEAR LOADING

In the skew-symmetric problem, the unknown functions in equations (38) and (39) can also be expressed in terms of a single unknown B(s,p) in accordance with the following relationships:

$$A^{(1)}(s,p) = -\frac{B(s,p)}{\Delta_{II}}\left[s\gamma_{21}(\beta^{(2)} - \beta^{(4)}e^{-2\gamma_{21}h}) + \frac{1}{2}(s^2+\gamma_{21}^2)e^{-(\gamma_{11}+\gamma_{21})h}\right]$$

$$A^{(2)}(s,p) = \frac{B(s,p)}{\Delta_{II}}\left[s\gamma_{21}e^{-2\gamma_{11}h}(\beta^{(1)} - \beta^{(3)}e^{-2\gamma_{21}h}) + \frac{1}{2}(s^2+\gamma_{21}^2)e^{-(\gamma_{11}+\gamma_{21})h}\right]$$

$$B^{(1)}(s,p) = -\beta^{(1)}e^{-(\gamma_{11}-\gamma_{21})h}A^{(1)}(s,p) - \beta^{(2)}e^{(\gamma_{11}+\gamma_{21})h}A^{(2)}(s,p)$$

$$B^{(2)}(s,p) = -\beta^{(3)}e^{-(\gamma_{11}+\gamma_{21})h}A^{(1)}(s,p) - \beta^{(4)}e^{(\gamma_{11}-\gamma_{21})h}A^{(2)}(s,p)$$

$$C^{(1)}(s,p) = \frac{e^{\gamma_{12}h}}{s^2-\gamma_{12}\gamma_{22}}\left[(s^2-\gamma_{11}\gamma_{22})e^{-\gamma_{11}h}A^{(1)}(s,p) + (s^2+\gamma_{11}\gamma_{22})e^{\gamma_{11}h}A^{(2)}(s,p) - s(\gamma_{21}-\gamma_{22})e^{-\gamma_{21}h}B^{(1)}(s,p) + s(\gamma_{21}+\gamma_{22})e^{\gamma_{21}h}B^{(2)}(s,p)\right]$$

$$C^{(2)}(s,p) = \frac{e^{\gamma_{22}h}}{s^2-\gamma_{21}\gamma_{22}} [s(\gamma_{12}-\gamma_{11})e^{-\gamma_{11}h} A^{(1)}(s,p) \tag{III.1}$$

$$+ s(\gamma_{12}+\gamma_{11})e^{\gamma_{11}h} A^{(2)}(s,p) + (s^2-\gamma_{21}\gamma_{12})e^{-\gamma_{21}h} B^{(1)}(s,p)$$

$$+ (s^2+\gamma_{21}\gamma_{12})e^{\gamma_{21}h} B^{(2)}(s,p)]$$

where Δ_{II} is given by equation (42).

ACKNOWLEDGEMENTS

This research was performed under Grant No. NSG-3179 supported by the National Aeronautics and Space Administration, Lewis Research Center, Cleveland, Ohio. The financial support of NASA and the encouragement of Dr. C. C. Chamis are gratefully acknowledged.

Dr. E. P. Chen's contribution to this work is also acknowledged. He has recently left Lehigh University and joined the staff at the Sandia Laboratories in Albuquerque, New Mexico.

REFERENCES

[1] "Linear Fracture Mechanics", edited by G. C. Sih, R. P. Wei and F. Erdogan, Envo Publishing Co., Inc., Bethlehem, Pa., 1975.

[2] Sih, G. C., Chen, E. P., Huang, S. L. and McQuillen, E. J., "Material Characterization on the Fracture of Filament-Reinforced Composites", J. of Composite Materials, Vol. 9, pp. 167-186, 1975.

[3] Sih, G. C., "Dynamic Crack Problems: Strain Energy Density Fracture Theory", Mechanics of Fracture, Vol. IV, edited by G. C. Sih, Sijthoff and Noordhoff International Publishing, Alphen, pp. XVII-XLVII, 1977.

[4] "Response of Metals and Metallic Structures to Dynamic Loading", Publication NMAB-341, National Academy of Sciences, Washington, D.C., 1978.

[5] Copson, E. T., "On Certain Dual Integral Equations", Proceedings of Glasgow Mathematical Association, Vol. 5, pp. 19-24, 1961.

[6] Chen, E. P. and Sih, G. C., "Transient Response of Cracks to Impact Loads", Mechanics of Fracture, Vol. IV, edited by G. C. Sih, Sijthoff and Noordhoff International Publishing, Alphen, pp. 1-58, 1977.

[7] Sih, G. C., Ravera, R. S. and Embley, G. T., "Impact Response of a Finite Crack in Plane Extension", International Journal of Solids and Structures, Vol. 8, pp. 977-993, 1972.

[8] Hilton, P. D. and Sih, G. C., "A Sandwiched Layer of Dissimilar Material Weakened by Crack-Like Imperfections", Proceedings of the 5th Southeastern Conference on Theoretical and Applied Mechanics.

[9] Papoulis, A., "A New Method of Inversion of the Laplace Transform", Quarterly of Applied Math., Vol. 14, pp. 405-414, 1957.

[10] Miller, M. K. and Guy, W. T., "Numerical Inversion of the Laplace Transform by Use of Jacobi Polynomials", SIAM Journal of Numerical Analysis, Vol. 3, pp. 624-635, 1966.

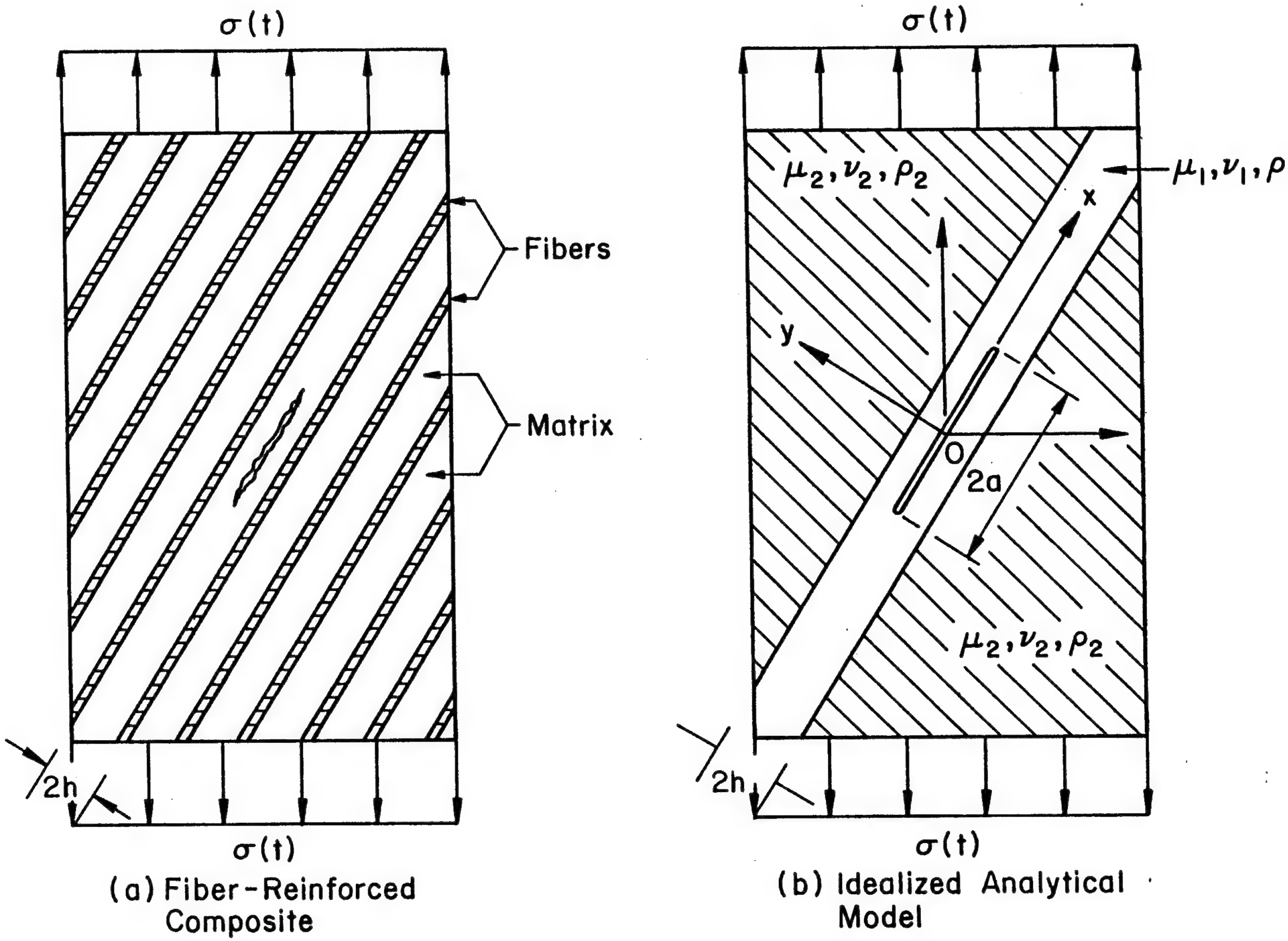

Figure 1. Fiber-reinforced unidirectional composite subjected to angle impact

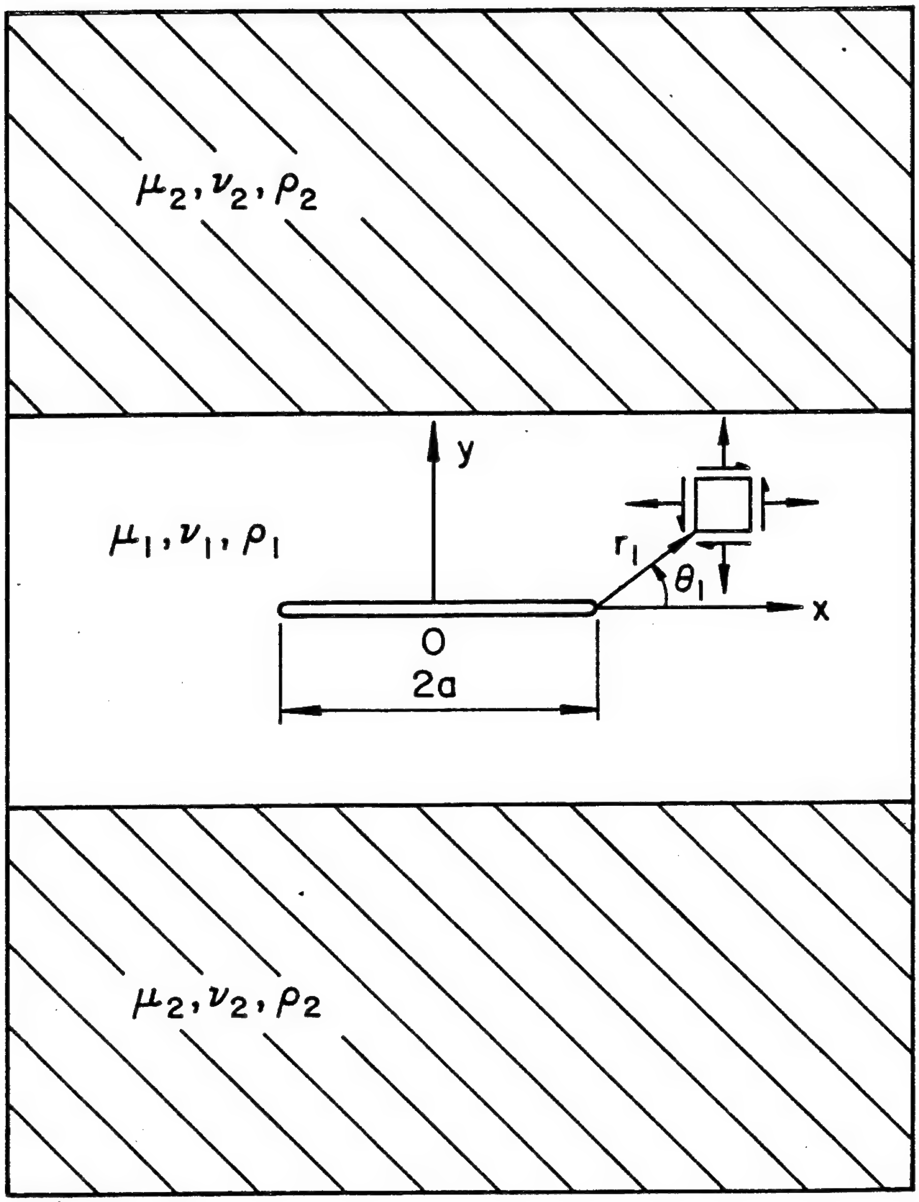

Figure 2. Stress element near crack in matrix of fiber-reinforced composite

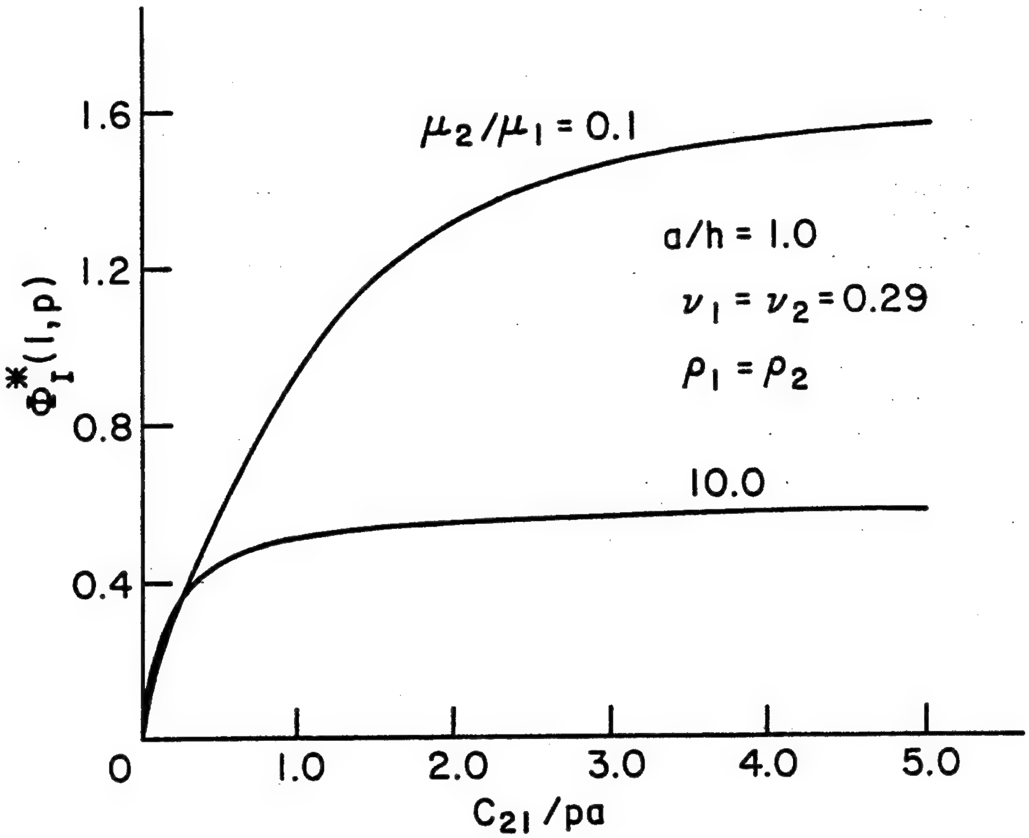

Figure 3. Variations of $\Phi_I^*(1,p)$ with c_{21}/pa for $a/h = 1.0$

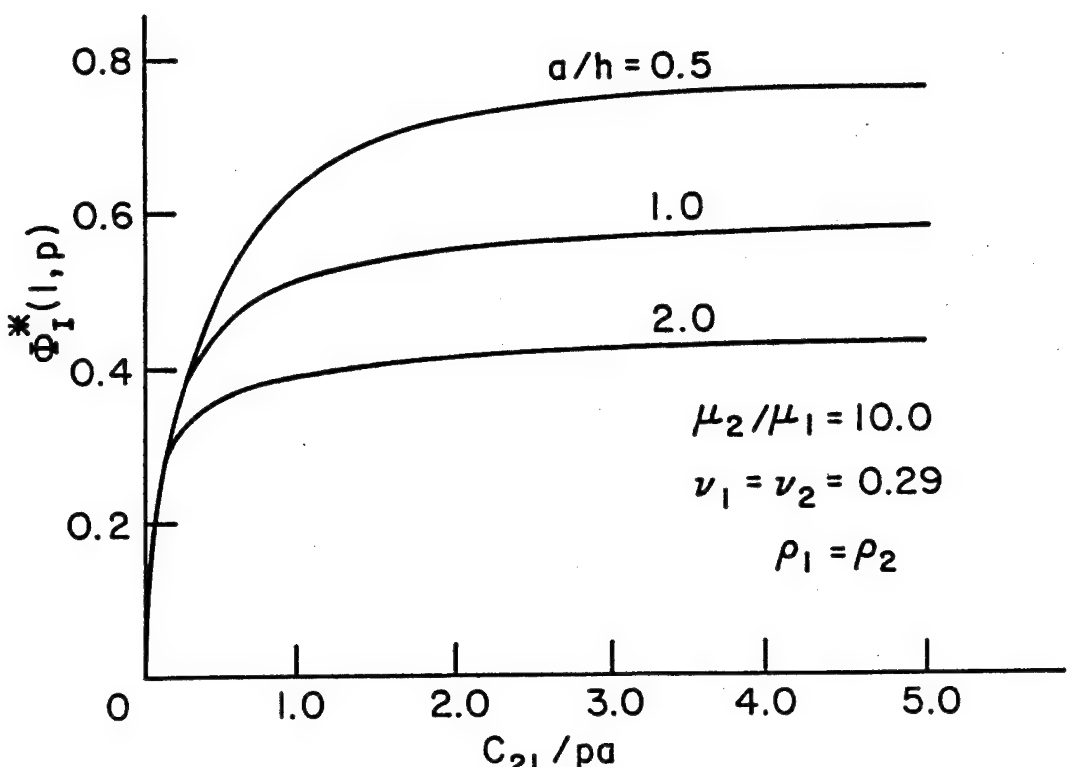

Figure 4. Variations of $\Phi_I^*(1,p)$ with c_{21}/pa for $\mu_2/\mu_1 = 10$

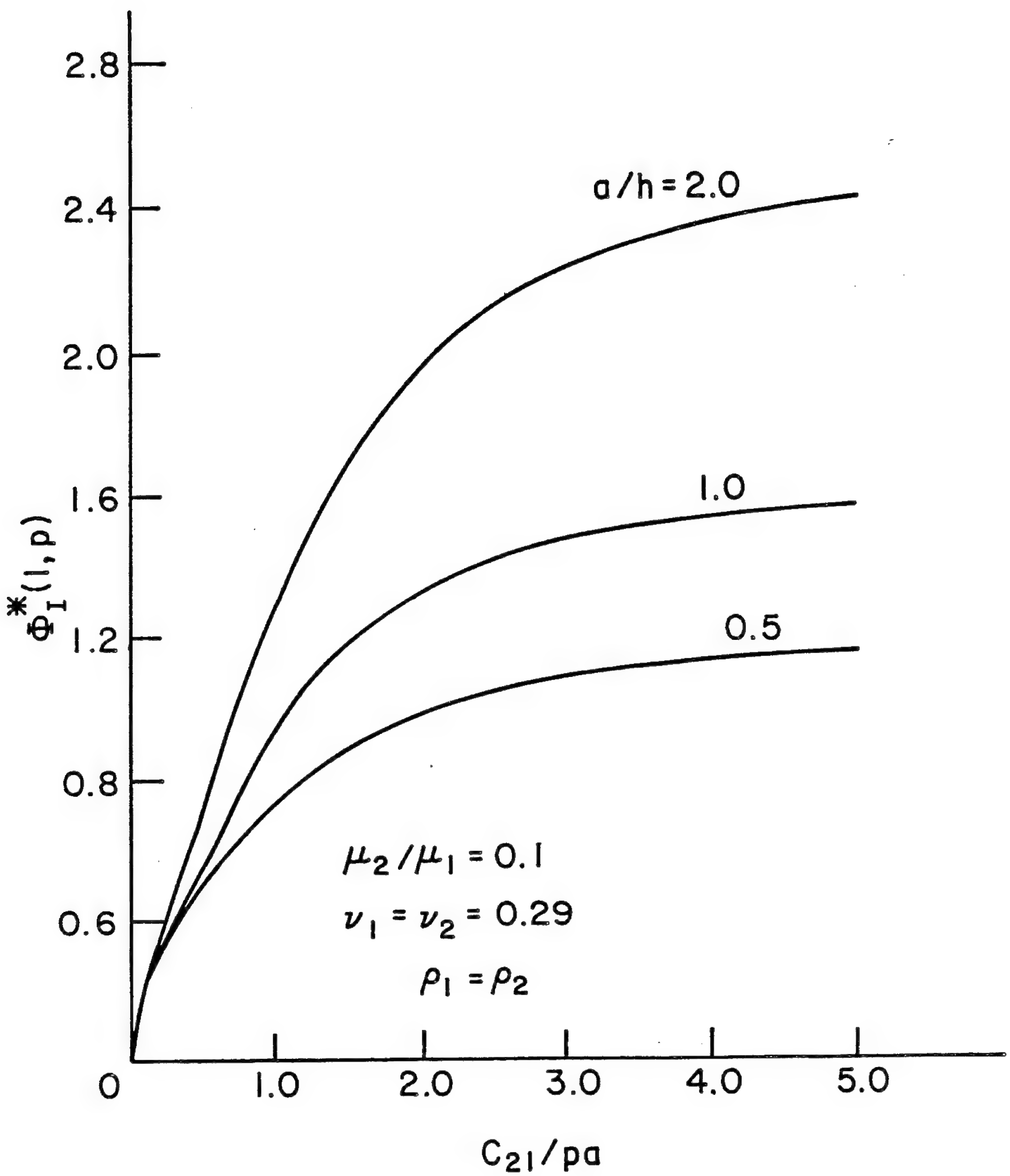

Figure 5. Variations of $\Phi_I^*(1,p)$ with c_{21}/pa for $\mu_2/\mu_1 = 0.1$

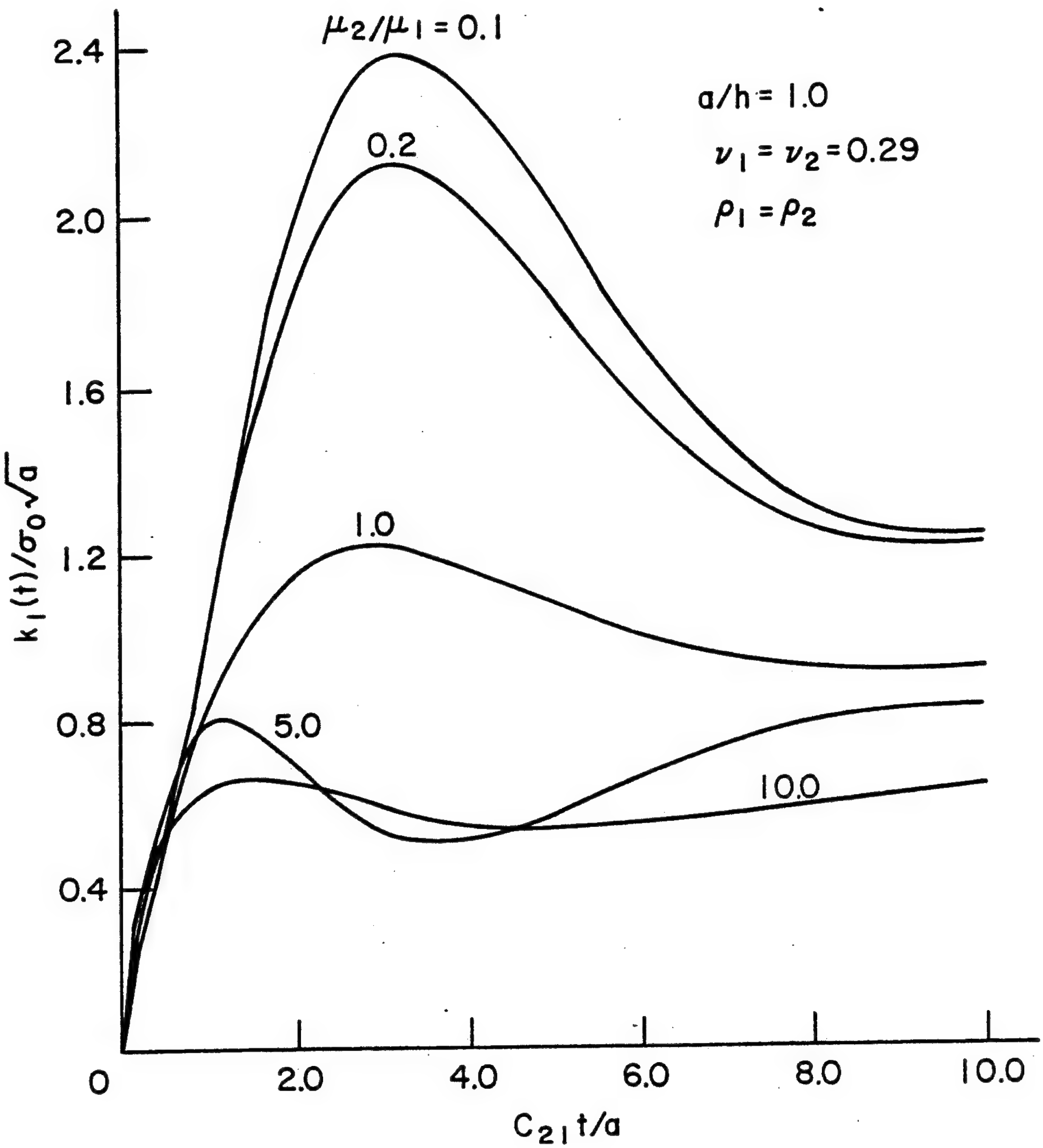

Figure 6. Dynamic stress intensity factor $k_1(t)$ versus time for $a/h = 1.0$

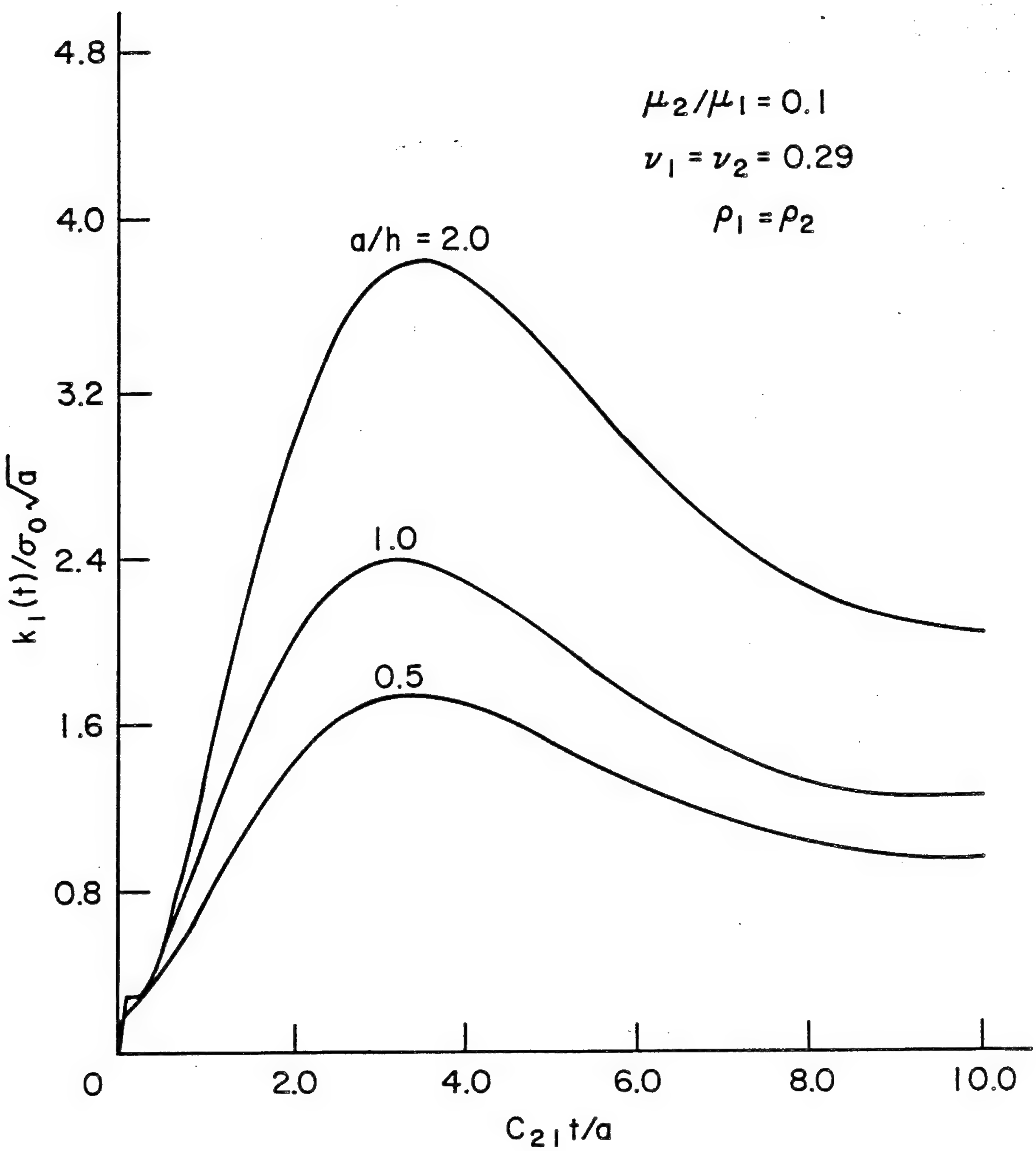

Figure 7. Dynamic stress intensity factor $k_1(t)$ versus time for $\mu_2/\mu_1 = 0.1$

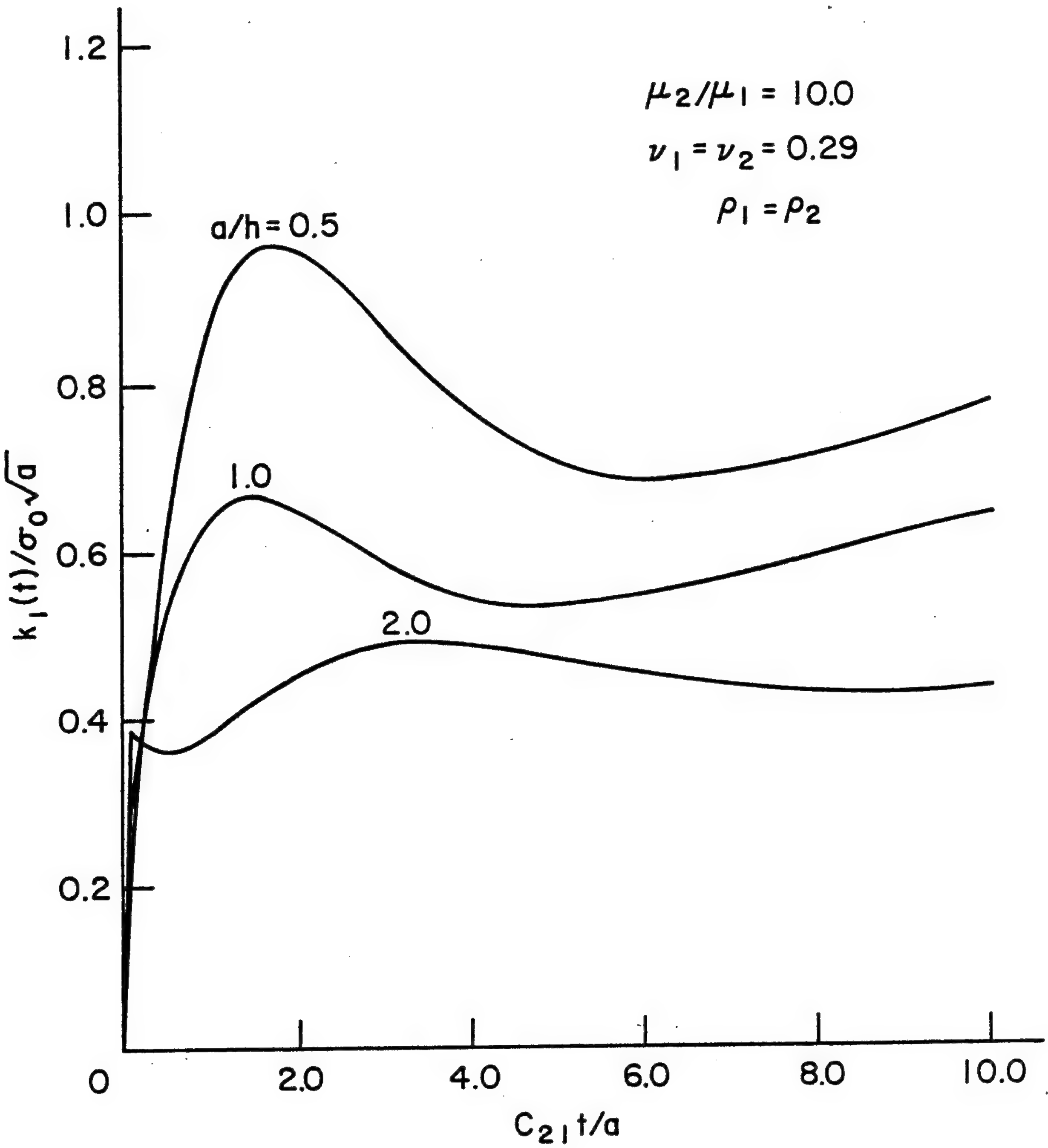

Figure 8. Dynamic stress intensity factor $k_1(t)$ versus time for $\mu_2/\mu_1 = 10.0$

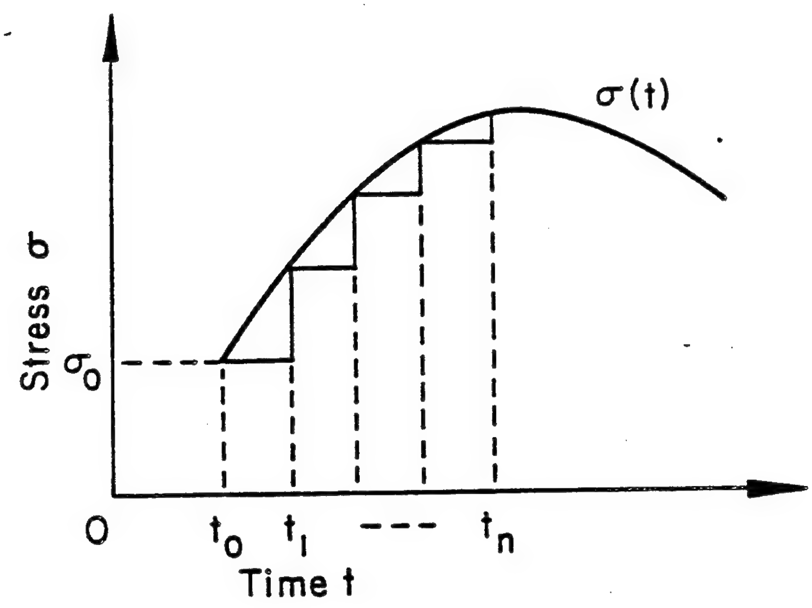

Figure 9. Applied stress as a general function of time

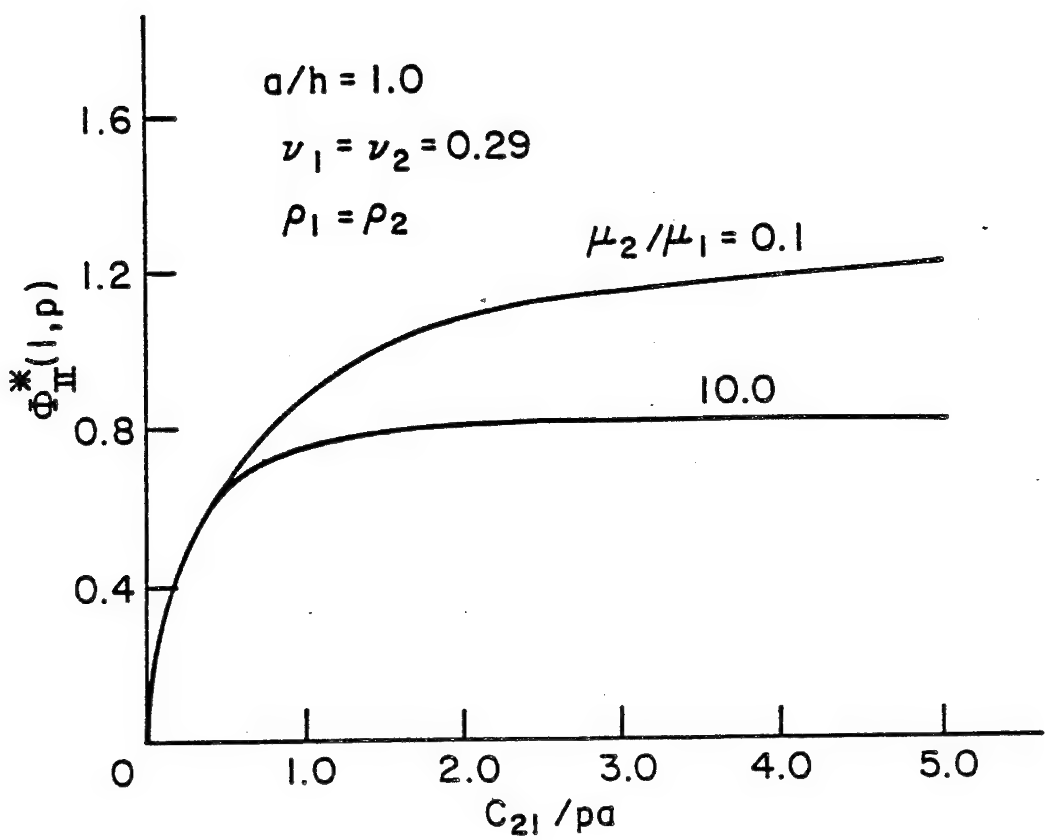

Figure 10. Variations of $\Phi^*_{II}(1,p)$ with c_{21}/pa

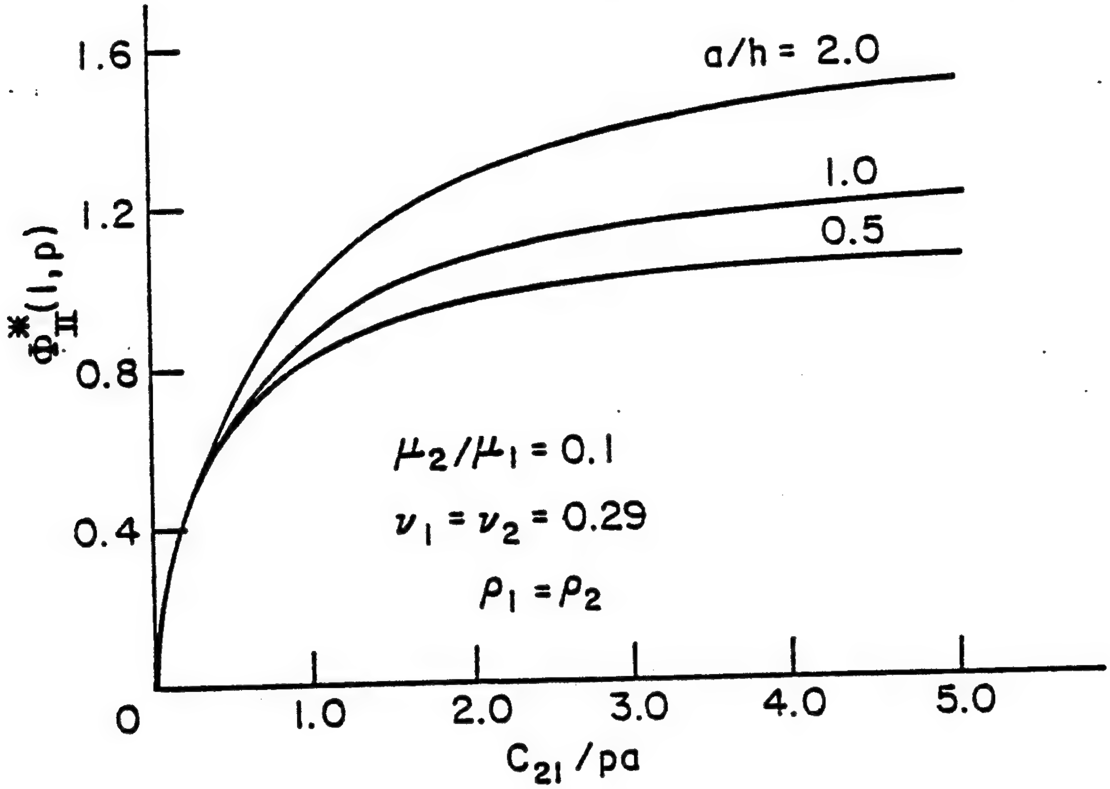

Figure 11. Variations of $\Phi^*_{II}(1,p)$ with c_{21}/pa

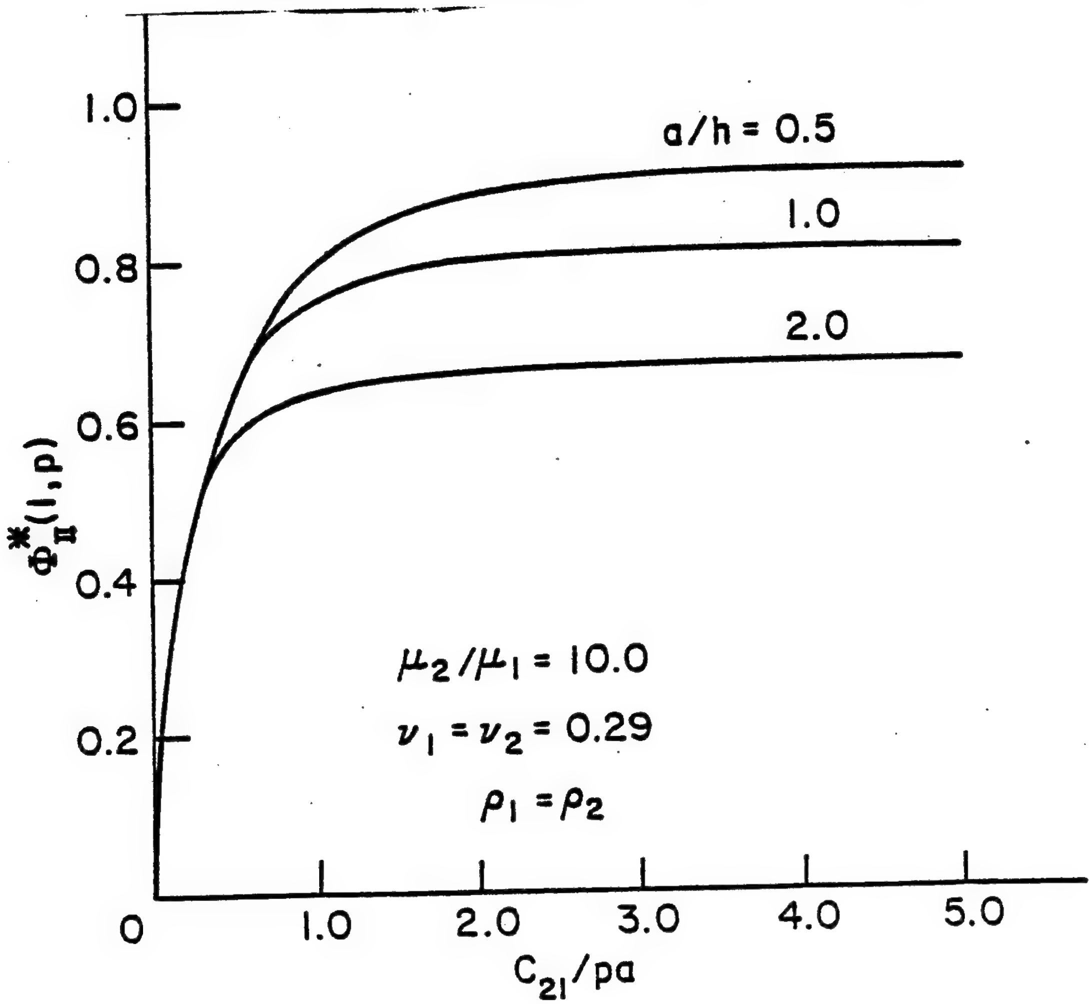

Figure 12. Variations of $\Phi^*_{II}(1,p)$ with c_{21}/pa

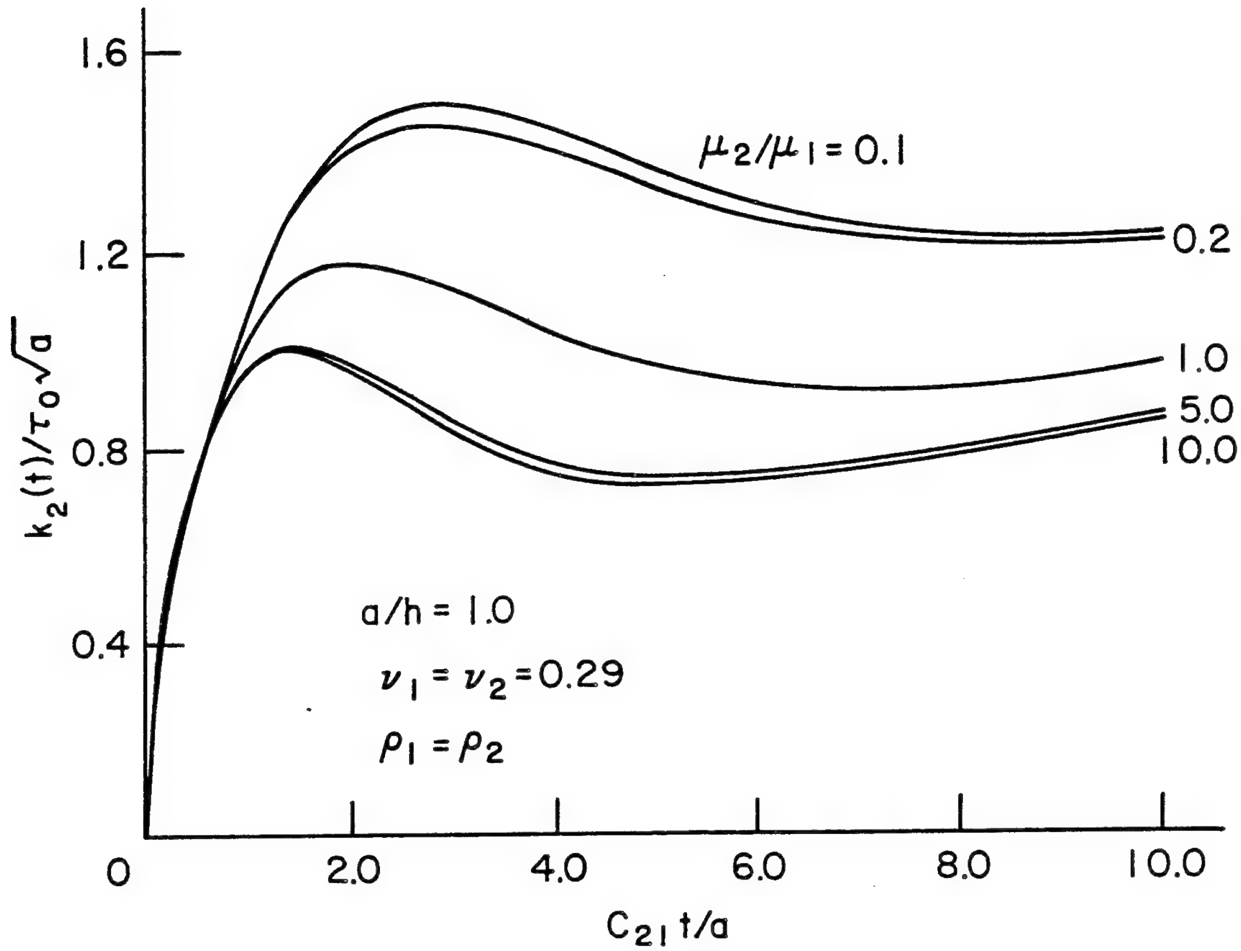

Figure 13. Dynamic stress intensity factor $k_2(t)$ versus time for a/h = 1.0

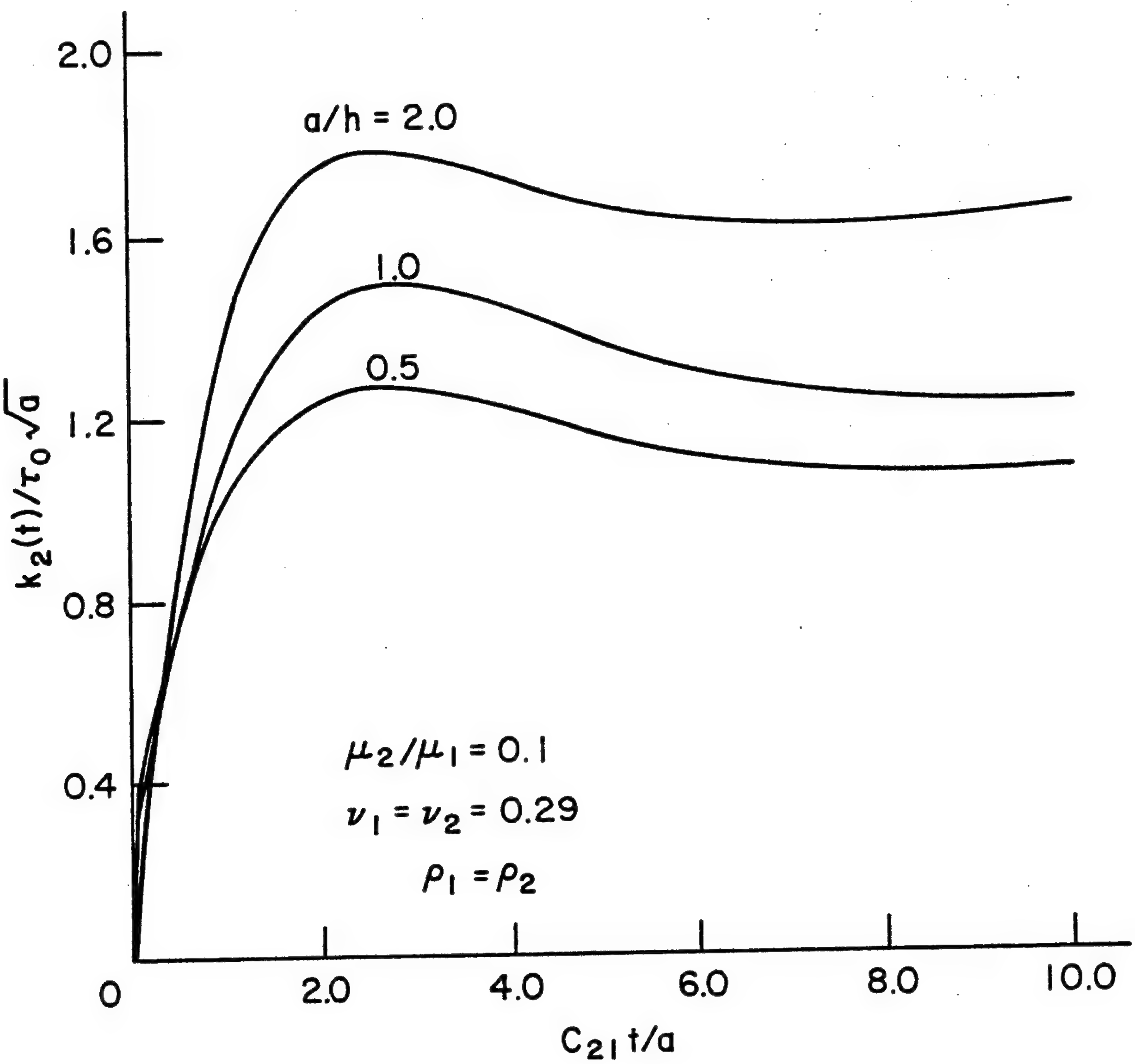

Figure 14. Dynamic stress intensity factor $k_2(t)$ versus time for $\mu_2/\mu_1 = 0.1$

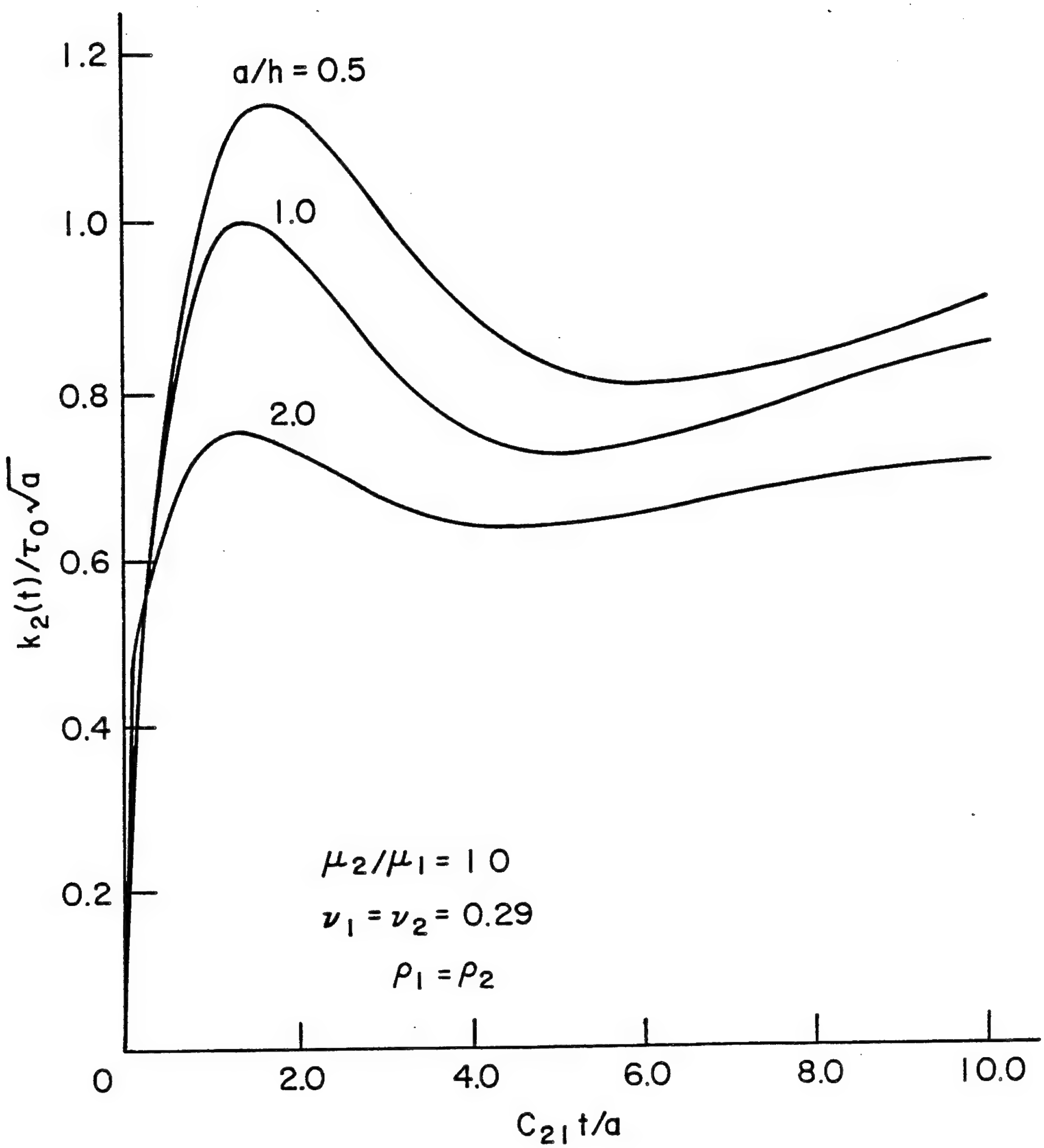

Figure 15. Dynamic stress intensity factor $k_2(t)$ versus time for $\mu_2/\mu_1 = 10.0$

Normal impact.

```
                PROGRAM BETA(INPUT,OUTPUT,PUNCH,PLOT,TAPE 99=PLOT)
  3             REAL NON(4),F(4,4,1),G(4,4),D(4),PT(4)
  3             REAL B(4),C(4)
  3             REAL LP(50),DTA(50)
  3             EQUIVALENCE (NON,B)
  3              COMMON K1,K2,K3,K4
  3             COMMON/AUX/H,P,PK1,PK2,BMU,X,Y
  3             LP(1)=0.0
  4             DTA(1)=0.0
  5             READ 2,K1,K2,K3,K4
 20           2 FORMAT(I2)
            * K1 = ORDER CF SYSTEM OF EQUATIONS
            * K2 = NO. OF DISTINCT KERNELS
            * K3 = NO. OF DATA POINTS
            * K4 = NO. OF DATA SETS TO BE EVALUATED
            * SET UP DATA POINTS
 20             AK=K3
 22             DO 5 N=1,K3
 23             AN=N
 24           5 PT(N)=AN/AK
            * SET UP INTEGRATION MATRIX
 31             M=K3-2
 33             N=K3-1
 34             A=K3
 35             A=1./(3.*A)
 37             DO 10 K=2,M,2
 41          10 D(K)=2.*A
 46             DO 15 K=1,N,2
 47          15 D(K)=4.*A
 54             D(K3)=A
            * CALCULATE NONHOMOGENEOUS TERMS
 56             RHS=1.0
 57             DO 22 I=1,K2
 61             PRINT 9
 64           9 FORMAT(1H1)
 64             READ 61,BMU
 72          61 FORMAT(F10.5)
 72             DO 999 II=1,K4
 74             DO 35 N=1,K3
 75          35 NON(N)=RHS*SQRT(PT(N))
            * CALCULATE KERNEL MATRICES
104             CALL CONST(I)
106             DO 20 N=1,K3
110             DO 20 M=1,K3
111             IF(M-N)25,30,30
114          25 F(M,N,I)=F(N,M,I)
123             GO TO 20
123          30 F(M,N,I)=FU(I,PT(M),PT(N))
134          20 CONTINUE
141             CALL CHANGE(F,G,D,I)
144             CALL LINEQ(G,B,C,    K3)
147              DO 40 L=1,K3
151             PRINT 6,PT(L),NON(L)
160           6 FORMAT(5X,F8.4,F15.6)
160          40 CONTINUE
163             LP(II+1)=NON(K3)
165             DTA(II+1)=P
167         999 CONTINUE
171             PUNCH 66,(DTA(IX),LP(IX),IX=1,19)
205          66 FORMAT(2F10.5)
205             CALL LAPINV(DTA,LP)
207          22 CONTINUE
212             END


                FUNCTION SIMF(I,A,B)
  6             COMMON/AUX/H,P,PK1,PK2,BMU,X,Y
  6             DEL=0.25*(B-A)
 10             IF(DEL)40,45,50
 12          45 SIMP=0.0
 13             RETURN
 14          50 CONTINUE
 14             SA=Z(I,A)+Z(I,B)
 26             SB=Z(I,A+2.*DEL)
 35             SC=Z(I,A+DEL)+Z(I,A+3.*DEL)
```

```
      S1=(DEL/3.)*(SA+2.*SB+4.*SC)
      IF(S1.EQ.0.0) GO TO 45
      K=8
   35 SB=SB+SC
      DEL=0.5*DEL
      SC=Z(I,A+DEL)
      J=K-1
      DO 5 N=3,J,2
      AN=N
    5 SC=SC+Z(I,A+AN*DEL)
      S2=(DEL/3.)*(SA+2.*SB+4.*SC)
      DIF=ABS((S2-S1)/S1)
      ER=0.01
      IF(DIF-ER) 30,25,25
   30 SIMP=S2
      RETURN
   25 K=2*K
      S1=S2
      IF(K-2048) 35,35,40
   40 PRINT 42,I,A,B
   42 FORMAT(5X,* INT. DOES NOT CONVERGE *,I3,2F9.4)
      PRINT 60,X,Y
   60 FORMAT(2F10.5)
      DO 70 J=1,10
      DIP=J
      DIP=DIP/10.
      W=Z(I,DIF)
      PRINT 60,W
   70 CONTINUE
      CALL EXIT
      END


      SUBROUTINE CHANGE(F,G,D,I)
      REAL F(4,4,1),G(4,4),D(4)
      COMMCN K1,K2,K3,K4
      DO 10 N=1,K3
      DO 10 M=1,K3
      G(M,N)   =F(M,N,I)*D(N)
   10 CONTINUE
      DO 20 N=1,K3
   20 G(N,N)=G(N,N)+1.0
      RETURN
      END


      SUBROUTINE LINEQ(A,B,T,N)
      REAL A(N,N),B(N),T(N)
      DO 5 I=2,N
    5 A(I,1)=A(I,1)/A(1,1)
      DO 10 K=2,N
      M=K-1
      DO 15 I=1,N
   15 T(I)=A(I,K)
      DO 20 J=1,M
      A(J,K)=T(J)
      J1=J+1
      DO 20 I=J1,N
      T(I)=T(I)-A(I,J)*A(J,K)
   20 CONTINUE
      A(K,K)=T(K)
      IF(K.EQ.N) GO TO 10
      M=K+1
      DO 25 I=M,N
   25 A(I,K)=T(I)/A(K,K)
   10 CONTINUE
*  BACK SUBSTITUTE
      DO 30 I=1,N
      T(I)=B(I)
      M=I+1
      IF(M.GT.N) GO TO 30
      DO 30 J=M,N
      B(J)=B(J)-A(J,I)*T(I)
   30 CONTINUE
      DO 35 I=1,N
```

```
      K=N+1-I
      B(K)=T(K)/A(K,K)
      K1=K-1
      IF(K1.EQ.0) GO TO 35
      DO 35 J1=1,K1
      J=K-J1
      T(J)=T(J)-A(J,K)*B(K)
   35 CONTINUE
      RETURN
      END
```

```
      FUNCTION BESJ0(A)
      IF(A-3.)5,5,10
    5 B=A*A/9.
      W=1.-2.2499997*B
      Z=B*B
      W=W+1.2656208*Z
      Z=Z*B
      W=W-.3163866*Z
      Z=Z*B
      W=W+.0444479*Z
      Z=Z*B
      W=W-.0039444*Z
      Z=Z*B
      BESJ0=W+.00021*Z
      RETURN
   10 B=3./A
      W=.79788456-.00000077*B
      V=A-.78539816-.04166397*B
      Z=B*B
      W=W-.0055274*Z
      V=V-.00003954*Z
      Z=Z*B
      W=W-.00009512*Z
      V=V+.00262573*Z
      Z=Z*B
      W=W+.00137237*Z
      V=V-.00054125*Z
      Z=Z*B
      W=W-.00072805*Z
      V=V-.00029333*Z
      Z=Z*B
      W=W+.00014476*Z
      V=V+.00013558*Z
      BESJ0=W/SQRT(A)*COS(V)
      RETURN
      END
```

```
      FUNCTION FU(I,A,B)
      COMMON/AUX/H,P,PK1,PK2,BMU,X,Y
      X=A
      Y=B
      IF(A*B)5,10,5
   10 FU=0.0
      RETURN
    5 SUM=SIMF(I,0.0,5.0)
      ER=0.01
      DEL =5.0
   20 UP=DEL+5.0
      ADDL=SIMF(I,DEL,UP)
      DEL =UP
      TEST=ABS(ADDL/SUM)
      SUM=SUM+ADDL
      IF(TEST-ER)15,20,20
   15 FU=SQRT(X*Y)*SUM
      RETURN
      END
```

```
              SUBROUTINE CONST(I)
   3          COMMON/ AUX/H,P,PK1,PK2,BMU,X,Y
   3          PR1=0.29
   5          PR2=0.29
   6          PK1=SQRT((1.-2.*PR1)/(2.*(1.-PR1)))
  15          PK2=SQRT((1.-2.*PR2)/(2.*(1.-PR2)))
  24          READ 1,P
  31        1 FORMAT(F10.5)
  31          HH=0.1
  33          HH=10.0
  34          HH=5.0
  36          HH=4.0
  37          HH=1.0
  41          HH=0.5
  42          HH=2.0
  44          H=1./HH
  45          PRINT 2,BMU,FR1,PR2,HH,P
  62        2 FORMAT(////5X,* MU2/MU1 =*F6.2,* NU1 =*F4.2,* NU2 =*F4.2///5X,* A
             1/H =*F4.2,* C21/PA =*F4.2)
  62          RETURN
  63          END


              FUNCTION Z(I,S)
   5          COMMON/ AUX/H,P,PK1,PK2,BMU,X,Y
   5          PP=P*P
   6          C1=PK1*PK1
  10          C2=PK2*PK2
  11          CC=1.-C1
  13          GA=SQRT(S*S+C1/PP)
  22          GB=SQRT(S*S+1./PP)
  31          GC=SQRT(S*S+C2/BMU/PP)
  40          GD=SQRT(S*S+1./BMU/FP)
  47          AA=S*S+1./PP/2.
  53          AB=1.-BMU
  54          AC=S*S-GC*GD
  57          AD=(GB-GD)/AC/PP/2.*BMU
  64          AE=(GB+GD)/AC/PP/2.*BMU
  71          AF=(S*S-GA*GD)/AC/PP/2.*BMU
  77          AG=(S*S+GA*GD)/AC/PP/2.*BMU
 105          AH=(S*S-GB*GC)/AC/PP/2.*BMU
 113          AI=(S*S+GB*GC)/AC/PP/2.*BMU
 121          AJ=(GA-GC)/AC/PP/2.*BMU
 126          AK=(GA+GC)/AC/PP/2.*BMU
 133          A1=-(AB*GB-AD)
 136          A2=AB*GB-AE
 140          A3=AA-BMU*S*S-AF
 145          A4=AA-BMU*S*S-AG
 150          A5=-AA+BMU*S*S+AH
 154          A6=-AA+BMU*S*S+AI
 157          A7=S*(AB*GA-AJ)
 162          A8=-S*(AB*GA-AK)
 165          BA=A1*A6-A2*A5
 170          BB=A3*A6-S*A2*A7
 173          BC=A4*A6-S*A2*A8
 176          BD=S*A1*A7-A3*A5
 202          BE=S*A1*A8-A4*A5
 205          B1=BB/BA
 207          B2=BC/BA
 211          B3=BD/BA
 212          B4=BE/BA
 214          EA=2.*GA*H
 216          EB=2.*GB*H
 220          EC=(EA+EB)/2.
 222          ED=2.*EC
 223          E1=EXP(-EA)
 226          E2=EXP(-EB)
 232          E3=EXP(-EC)
 236          E4=EXP(-ED)
 242          DL=B2+B3*E4+B4*E2+B1*E1
 251          D1=2.*PP/CC/GA/DL
 255          D2=AA*AA-S*S*GA*GB
 263          D3=B2-B3*E4
 266          D4=2.*AA*(GB*(B1*B4-B2*B3)-S*S*GA)*E3
 275          D5=(AA*AA+S*S*GA*GB)*(B4*E2-B1*E1)
```

```
      F=D1*(D2*D3+D4+D5)
      Z=(F-S)*BESJO(S*X)*BESJO(S*Y)
      RETURN
      END

      SUBROUTINE LAPINV(GLAM,PHI)
C     THIS PROGRAM EVALUATES THE COEFFICIENTS FOR SERIES
C     OF JACOBI POLYNOMIALS WHICH REPRESENTS A LAPLACE
C     INVERSION INTEGRAL
      REAL MUL
      DIMENSION A(50),GLAM(50),PHI(50),C(4,50)
      DIMENSION BK(101),TT(101)
      COMMON/2/TI,TF,DT,MN,BK,TT
      READ 1,NN,MN,MM
    1 FORMAT(3I2)
      READ 2,TI,TF,DT
    2 FORMAT(3F10.5)
      PRINT 99
   99 FORMAT(1H1)
      CALL SPLICE(GLAM,PHI,MM,C)
      PRINT 101
  101 FORMAT(////5X,*   GLAM                PHI      *)
      PRINT 102,(GLAM(I),PHI(I),I=1,MM)
  102 FORMAT(5X,F10.5,5X,F10.5)
      M11=MM-1
      PRINT 300
  300 FORMAT(////5X,*    C(1,J)            C(2,J)             C(3,J)             C
     1,J)  *)
      PRINT 103,((C(I,J),I=1,4),J=1,M11)
  103 FORMAT(5X,F10.5,5X,F10.5,5X,F10.5,5X,F10.5)
      PRINT 99
      DO 10 I=1,NN
      READ 3,BET,DEL
    3 FORMAT(2F10.5)
      PRINT 98,BET,DEL
   98 FORMAT(/////5X,*BETA =*F5.3,* DELTA =*F5.3)
      DO 11 L=1,MN
      AL=L
      S=1./(AL+BET)/DEL
      CALL SPLINE(GLAM,PHI,MM,C,S,G)
      F=G*S
      IF(AL-2.)81,82,83
   81 A(1)=(1.+BET)*DEL*F
      GO TO 11
   82 A(2)=((2.+BET)*DEL*F-A(1))*(3.+BET)
      GO TO 11
   83 CONTINUE
      TOP=1.
      L1=L-1
      AL1=L1
      DO 12 J=1,L1
      AJ=J
      TOP=AJ*TOP
   12 CONTINUE
      L2=2*L-1
      BOT=1.
      DO 13 J=L,L2
      AJ=J
      BOT=(AJ+BET)*BOT
   13 CONTINUE
      MUL=BOT/TOP
      SUM=0.0
      DO 14 N=1,L1
      AN=N
      IF(AN-2.)85,86,87
   85 TOD=1.
      GO TO 88
   86 TOD=AL1
      GO TO 88
   87 CONTINUE
      TOD=1.
      ICH=L1-(N-2)
      DO 15 J=ICH,L1
      AJ=J
      TOD=AJ*TOD
```

```
   15 CONTINUE
   88 CONTINUE
      BOC=1.
      JA=L1+N
      DO 16 J=L,JA
      AJ=J
      BOD=BOD*(AJ+BET)
   16 CONTINUE
      CO=TOD/BOD
      SUM=SUM+CO*A(N)
   14 CONTINUE
      A(L)=MUL*(DEL*F-SUM)
   11 CONTINUE
      CALL JACSER(DEL,A,BET)
      CALL NAMPLT
      CALL QIKSET(6.0,0.0,0.0,6.0,0.0,0.0)
      CALL QIKSAX(3,3)
      CALL QIKPLT(TT,BK,101)
      CALL ENDPLT
   10 CONTINUE
  999 CONTINUE
      RETURN
      END


      SUBROUTINE JACSER(D,C,B)
      DIMENSICN C(50),SF(50),P(50)
      DIMENSION BK(101),TT(101)
      COMMON/2/TI,TF,DT,MN,BK,TT
      TT(1)=0.0
      BK(1)=0.0
      LM=1
      T=TI
   12 T=T+DT
      X=2.*EXP(-D*T)-1.
      CALL JACOBI(MN,X,B,P)
      SF(1)=C(1)*P(1)
      DO 10 L=2,MN
      L1=L-1
      AL=L
      SF(L)=SF(L1)+C(L)*F(L)
   10 CONTINUE
      PRINT 97,T,X
   97 FORMAT(/////5X,*  T =*F6.3,*   X =*F10.5)
      PRINT 96
   96 FORMAT(///5X,* I    C(I)     *,5X,* N    F(T)     *)
      DO 11 I=1,6
      PRINT 95,I,C(I),I,SF(I)
   95 FORMAT(5X,I2,F10.2,5X,I2,F10.5)
   11 CONTINUE
      LM=LM+1
      BK(LM)=SF(5)
      TT(LM)=T
      IF(T.LE.TF) GO TO 12
      RETURN
      END


      SUBROUTINE JACOBI(N,X,B,PB)
C     THIS PROGRAM CALCULATES JACOBI POLYNOMIALS OF ORDER
C     K-1 WITH ARG X AND PARAMETER B GT -1
      DIMENSICN PB(N)
      AN=N
      IF(AN-2.)1,2,3
    1 PB(1)=1.
      RETURN
    2 PB(1)=1.
      PB(2)=X-B*(1.-X)/2.
      RETURN
    3 BSQ=B*B
      BONE=B+1.
      PB(1)=1.
      PB(2)=X-B*(1.-X)/2.
      DO 4 K=3,N
      AK=K
```

```
      AK1=AK-1.
      AK2=AK-2.
      K1=K-1
      K2=K-2
      CO1=((2.*AK1)+B)*X
      CO1=((2.*AK2)+B)*CO1
      CO1=((2.*AK2)+BONE)*(CO1-BSQ)
      CO2=2.*AK2*(AK2+B)*((2.*AK1)+B)
      CO=2.*AK1*(AK1+B)*((2.*AK2)+B)
    4 PB(K)=(CO1*PB(K1)-CO2*PB(K2))/CO
      RETURN
      END


      SUBROUTINE SPLINE(X,Y,M,C,XINT,YINT)
      DIMENSION X(50),Y(50),C(4,50)
      IF(XINT-X(1))1,10,11
   10 YINT=Y(1)
      RETURN
   11 CONTINUE
      IF(X(M)-XINT)1,12,13
   12 YINT=Y(M)
      RETURN
   13 CONTINUE
      K=M/2
      N=M
    2 CONTINUE
      IF(X(K)-XINT)3,14,5
   14 YINT=Y(K)
      RETURN
    3 CONTINUE
      IF(XINT-X(K+1))4,15,7
   15 YINT=Y(K+1)
      RETURN
    4 CONTINUE
      YINT=(X(K+1)-XINT)*(C(1,K)*(X(K+1)-XINT)**2+C(3,K))
      YINT=YINT+(XINT-X(K))*(C(2,K)*(XINT-X(K))**2+C(4,K))
      RETURN
    5 CONTINUE
      IF(X(K-1)-XINT)6,16,17
    6 K=K-1
      GO TO 4
   16 YINT=Y(K-1)
      RETURN
   17 N=K
      K=K/2
      GO TO 2
    7 LL=K
      K=(N+K)/2
    8 CONTINUE
      IF(X(K)-XINT)3,14,18
   18 CONTINUE
      IF(X(K-1)-XINT)6,16,19
   19 N=K
      K=(LL+K)/2
      GO TO 8
    1 PRINT 101
  101 FORMAT(* OUT OF RANGE FOR INTERPOLATION  *)
      STOP
      END


      SUBROUTINE SPLICE(X,Y,M,C)
      DIMENSION X(50),Y(50),D(50),P(50),E(50),C(4,50)
      DIMENSION A(50,3),B(50),Z(50)
      MM=M-1
      DO 2 K=1,MM
      D(K)=X(K+1)-X(K)
      P(K)=D(K)/6.
    2 E(K)=(Y(K+1)-Y(K))/D(K)
      DO 3 K=2,MM
    3 B(K)=E(K)-E(K-1)
      A(1,2)=-1.-D(1)/D(2)
      A(1,3)=D(1)/D(2)
      A(2,3)=P(2)-P(1)*A(1,3)
```

```
    44          A(2,2)=2.*(P(1)+P(2))-P(1)*A(1,2)
    50          A(2,3)=A(2,3)/A(2,2)
    51          B(2)=B(2)/A(2,2)
    53          DO 4 K=3,MM
    54          A(K,2)=2.*(P(K-1)+P(K))-P(K-1)*A(K-1,3)
    61          B(K)=B(K)-P(K-1)*B(K-1)
    65          A(K,3)=P(K)/A(K,2)
    70        4 B(K)=B(K)/A(K,2)
    74          Q=D(M-2)/D(M-1)
    76          A(M,1)=1.+Q+A(M-2,3)
   101          A(M,2)=-Q-A(M,1)*A(M-1,3)
   105          B(M)=B(M-2)-A(M,1)*B(M-1)
   112          Z(M)=B(M)/A(M,2)
   114          MN=M-2
   116          DO 6 I=1,MN
   117          K=M-I
   120        6 Z(K)=B(K)-A(K,3)*Z(K+1)
   127          Z(1)=-A(1,2)*Z(2)-A(1,3)*Z(3)
   133          DO 7 K=1,MM
   135          Q=1./(6.*D(K))
   140          C(1,K)=Z(K)*Q
   143          C(2,K)=Z(K+1)*Q
   146          C(3,K)=Y(K)/D(K)-Z(K)*P(K)
   154        7 C(4,K)=Y(K+1)/D(K)-Z(K+1)*P(K)
   165          RETURN
   165          END
```

Shear impact

```
      PROGRAM BETA(INPUT,OUTPUT,PUNCH,PLOT,TAPE 99=PLOT)
      REAL NON(4),F(4,4,1),G(4,4),D(4),PT(4)
      REAL B(4),C(4)
      REAL LP(50),DTA(50)
      EQUIVALENCE (NON,B)
       COMMON K1,K2,K3,K4
      COMMON/AUX/H,P,PK1,PK2,BMU,X,Y
      LP(1)=0.0
      DTA(1)=0.0
      READ 2,K1,K2,K3,K4
    2 FORMAT(I2)
*   K1 = ORDER OF SYSTEM OF EQUATIONS
*   K2 = NO. OF DISTINCT KERNELS
*   K3 = NO. OF DATA POINTS
*   K4 = NO. OF DATA SETS TO BE EVALUATED
*   SET UP DATA POINTS
      AK=K3
      DO 5 N=1,K3
      AN=N
    5 PT(N)=AN/AK
*   SET UP INTEGRATION MATRIX
      M=K3-2
      N=K3-1
      A=K3
      A=1./(3.*A)
      DO 10 K=2,M,2
   10 D(K)=2.*A
      DO 15 K=1,N,2
   15 D(K)=4.*A
      D(K3)=A
*   CALCULATE NONHOMOGENEOUS TERMS
      RHS=1.0
      DO 22 I=1,K2
      PRINT 9
    9 FORMAT(1H1)
      READ 61,BMU
   61 FORMAT(F10.5)
      DO 999 II=1,K4
      DO 35 N=1,K3
   35 NON(N)=RHS*SQRT(PT(N))
*   CALCULATE KERNEL MATRICES
      CALL CONST(I)
      DO 20 N=1,K3
      DO 20 M=1,K3
      IF(M-N)25,30,30
   25 F(M,N,I)=F(N,M,I)
      GO TO 20
   30 F(M,N,I)=FU(I,PT(M),PT(N))
   20 CONTINUE
      CALL CHANGE(F,G,D,I)
      CALL LINEQ(G,B,C,     K3)
       DO 40 L=1,K3
      PRINT 6,PT(L),NON(L)
    6 FORMAT(5X,F8.4,F15.6)
   40 CONTINUE
      LP(II+1)=NON(K3)
      DTA(II+1)=P
  999 CONTINUE
      PUNCH 66,(DTA(IX),LP(IX),IX=1,19)
   66 FORMAT(2F10.5)
      CALL LAPINV(DTA,LP)
   22 CONTINUE
      END


      FUNCTION SIMP(I,A,B)
      COMMON/AUX/H,P,PK1,PK2,BMU,X,Y
      DEL=0.25*(B-A)
      IF(DEL)40,45,50
   45 SIMP=0.0
      RETURN
   50 CONTINUE
      SA=Z(I,A)+Z(I,B)
      SB=Z(I,A+2.*DEL)
      SC=Z(I,A+DEL)+Z(I,A+3.*DEL)
```

```
      S1=(DEL/3.)*(SA+2.*SB+4.*SC)
      IF(S1.EQ.0.0) GO TO 45
      K=8
   35 SB=SB+SC
      DEL=0.5*DEL
      SC=Z(I,A+DEL)
      J=K-1
      DO 5 N=3,J,2
      AN=N
    5 SC=SC+Z(I,A+AN*DEL)
      S2=(DEL/3.)*(SA+2.*SB+4.*SC)
      DIF=ABS((S2-S1)/S1)
      ER=0.01
      IF(DIF-ER)30,25,25
   30 SIMP=S2
      RETURN
   25 K=2*K
      S1=S2
      IF(K-2048)35,35,40
   40 PRINT 42,I,A,B
   42 FORMAT(5X,* INT. DOES NOT CONVERGE *,I3,2F9.4)
      PRINT 60,X,Y
   60 FORMAT(2F10.5)
      DO 70 J=1,10
      DIP=J
      DIP=DIP/10.
      W=Z(I,DIP)
      PRINT 60,W
   70 CONTINUE
      CALL EXIT
      END
```

```
      SUBROUTINE CHANGE(F,G,D,I)
      REAL F(4,4,1),G(4,4),D(4)
      COMMON K1,K2,K3,K4
      DO 10 N=1,K3
      DO 10 M=1,K3
      G(M,N)  =F(M,N,I)*D(N)
   10 CONTINUE
      DO 20 N=1,K3
   20 G(N,N)=G(N,N)+1.0
      RETURN
      END
```

```
      SUBROUTINE LINEQ(A,B,T,N)
      REAL A(N,N),B(N),T(N)
      DO 5 I=2,N
    5 A(I,1)=A(I,1)/A(1,1)
      DO 10 K=2,N
      M=K-1
      DO 15 I=1,N
   15 T(I)=A(I,K)
      DO 20 J=1,M
      A(J,K)=T(J)
      J1=J+1
      DO 20 I=J1,N
      T(I)=T(I)-A(I,J)*A(J,K)
   20 CONTINUE
      A(K,K)=T(K)
      IF(K.EQ.N) GO TO 10
      M=K+1
      DO 25 I=M,N
   25 A(I,K)=T(I)/A(K,K)
   10 CONTINUE
*   BACK SUBSTITUTE
      DO 30 I=1,N
      T(I)=B(I)
      M=I+1
      IF(M.GT.N) GO TO 30
      DO 30 J=M,N
      B(J)=B(J)-A(J,I)*T(I)
   30 CONTINUE
      DO 35 I=1,N
```

```
      K=N+1-I
      B(K)=T(K)/A(K,K)
      K1=K-1
      IF(K1.EQ.0) GO TO 35
      DO 35 J1=1,K1
      J=K-J1
      T(J)=T(J)-A(J,K)*B(K)
   35 CONTINUE
      RETURN
      END


      FUNCTION BESJO(A)
      IF(A-3.)5,5,10
    5 B =A*A/9.
      W=1.-2.2499997*B
      Z=B*B
      W=W+1.2656208*Z
      Z=Z*B
      W=W-.3163866*Z
      Z=Z*B
      W=W+.0444479*Z
      Z=Z*B
      W=W-.0039444*Z
      Z =Z*B
      BESJO=W+.00021*Z
      RETURN
   10 B=3./A
      W=.79788456-.00000077*B
      V=A-.78539816-.04166397*B
      Z=B*B
      W=W-.0055274*Z
      V=V-.00003954*Z
      Z=Z*B
      W=W-.00009512*Z
      V=V+.00262573*Z
      Z =Z*B
      W=W+.00137237*Z
      V=V-.00054125*Z
      Z=Z*B
      W=W-.00072805*Z
      V=V-.00029333*Z
      Z =Z*B
      W=W+.00014476*Z
      V=V+.00013558*Z
      BESJO=W/SQRT(A)*COS(V)
      RETURN
      END


      FUNCTION FU(I,A,B)
      COMMON/AUX/H,P,PK1,PK2,BMU,X,Y
      X=A
      Y=B
      IF(A*B)5,10,5
   10 FU=0.0
      RETURN
    5 SUM=SIMP(I,0.0,5.0)
      ER=0.01
      DEL =5.0
   20 UP=DEL+5.0
      ADDL=SIMP(I,DEL,UP)
      DEL =UP
      TEST=ABS(ADDL/SUM)
      SUM=SUM+ADDL
      IF(TEST-ER)15,20,20
   15 FU=SQRT(X*Y)*SUM
      RETURN
      END
```

```
          SUBROUTINE CONST(I)
  3       COMMON/AUX/H,P,PK1,PK2,BMU,X,Y
  3       PR1=0.29
  5       PR2=0.29
  6       PK1=SQRT((1.-2.*PR1)/(2.*(1.-PR1)))
 15       PK2=SQRT((1.-2.*PR2)/(2.*(1.-PR2)))
 24       READ 1,P
 31     1 FORMAT(F10.5)
 31       HH=0.1
 33       HH=10.0
 34       HH=5.0
 36       HH=4.0
 37       HH=0.5
 41       HH=1.0
 42       HH=2.0
 44       H=1./HH
 45       PRINT 2,BMU,PR1,PR2,HH,P
 62     2 FORMAT(////5X,* MU2/MU1 =*F6.2,* NU1 =*F4.2,* NU2 =*F4.2///5X,* A
         1/H =*F4.2,* C21/PA =*F4.2)
 62       RETURN
 63       END


          FUNCTION Z(I,S)
  5       COMMON/AUX/H,P,PK1,PK2,BMU,X,Y
  5       PP=P*P
  6       C1=PK1*PK1
 10       C2=PK2*PK2
 11       CC=1.-C1
 13       GA=SQRT(S*S+C1/PP)
 22       GB=SQRT(S*S+1./PP)
 31       GC=SQRT(S*S+C2/BMU/PP)
 40       GD=SQRT(S*S+1./BMU/PP)
 47       AA=S*S+1./PP/2.
 53       AB=1.-BMU
 54       AC=S*S-GC*GD
 57       AD=(GB-GD)/AC/PP/2.*BMU
 64       AE=(GB+GD)/AC/PP/2.*BMU
 71       AF=(S*S-GA*GD)/AC/PP/2.*BMU
 77       AG=(S*S+GA*GD)/AC/PP/2.*BMU
105       AH=(S*S-GB*GC)/AC/PP/2.*BMU
113       AI=(S*S+GB*GC)/AC/PP/2.*BMU
121       AJ=(GA-GC)/AC/PP/2.*BMU
126       AK=(GA+GC)/AC/PP/2.*BMU
133       A1=-(AB*GB-AD)
136       A2=AB*GB-AE
140       A3=AA-BMU*S*S-AF
145       A4=AA-BMU*S*S-AG
150       A5=-AA+BMU*S*S+AH
154       A6=-AA+BMU*S*S+AI
157       A7=S*(AB*GA-AJ)
162       A8=-S*(AB*GA-AK)
165       BA=A1*A6-A2*A5
170       BB=A3*A6-S*A2*A7
173       BC=A4*A6-S*A2*A8
176       BD=S*A1*A7-A3*A5
202       BE=S*A1*A8-A4*A5
205       B1=BB/BA
207       B2=BC/BA
211       B3=BD/BA
212       B4=BE/BA
214       EA=2.*GA*H
216       EB=2.*GB*H
220       EC=(EA+EB)/2.
222       ED=2.*EC
223       E1=EXP(-EA)
226       E2=EXP(-EB)
232       E3=EXP(-EC)
236       E4=EXP(-ED)
242       DL=B2+B3*E4-B4*E2-B1*E1
251       D1=2.*PP/CC/GB/DL
255       D2=AA*AA-S*S*GA*GB
263       D3=B2-B3*E4
266       D4=2.*AA*(GB*(B1*B4-B2*B3)-S*S*GA)*E3
275       D5=(AA*AA+S*S*GA*GB)*(B4*E2-B1*E1)
```

```
306          F=D1*(D2*D3+D4+D5)*BESJO(S*Y)
313          Z=(F-S)*BESJO(S*X)*BESJO(S*Y)
330          RETURN
330          END

             SUBROUTINE LAPINV(GLAM,PHI)
      C      THIS PROGRAM EVALUATES THE COEFFICIENTS FOR SERIES
      C      OF JACOBI POLYNOMIALS WHICH REPRESENTS A LAPLACE
      C      INVERSION INTEGRAL
  5          REAL MUL
  5          DIMENSION A(50),GLAM(50),PHI(50),C(4,50)
  5          DIMENSION BK(101),TT(101)
  5          COMMON/2/TI,TF,DT,MN,BK,TT
  5          READ 1,NN,MN,MM
 16        1 FORMAT(3I2)
 16          READ 2,TI,TF,DT
 30        2 FORMAT(3F10.5)
 30          PRINT 99
 34       99 FORMAT(1H1)
 34          CALL SPLICE(GLAM,PHI,MM,C)
 40          PRINT 101
 44      101 FORMAT(////5X,*   GLAM                PHI      *)
 44          PRINT 102,(GLAM(I),PHI(I),I=1,MM)
 65      102 FORMAT(5X,F10.5,5X,F10.5)
 65          M11=MM-1
 67          PRINT 300
 73      300 FORMAT(////5X,*    C(1,J)            C(2,J)            C(3,J)            C(
            1,J)  *)
 73          PRINT 103,((C(I,J),I=1,4),J=1,M11)
112      103 FORMAT(5X,F10.5,5X,F10.5,5X,F10.5,5X,F10.5)
112          PRINT 99
116          DO 10 I=1,NN
121          READ 3,BET,DEL
130        3 FORMAT(2F10.5)
130          PRINT 98,BET,DEL
140       98 FORMAT(////5X,*BETA =*F5.3,* DELTA =*F5.3)
140          DO 11 L=1,MN
143          AL=L
144          S=1./(AL+BET)/DEL
150          CALL SPLINE(GLAM,PHI,MM,C,S,G)
153          F=G*S
155          IF(AL-2.)81,82,83
161       81 A(1)=(1.+BET)*DEL*F
165          GO TO 11
165       82 A(2)=((2.+BET)*DEL*F-A(1))*(3.+BET)
175          GO TO 11
175       83 CONTINUE
175          TOP=1.
177          L1=L-1
201          AL1=L1
202          DO 12 J=1,L1
203          AJ=J
204          TOP=AJ*TOP
206       12 CONTINUE
210          L2=2*L-1
212          BOT=1.
214          DO 13 J=L,L2
215          AJ=J
216          BOT=(AJ+BET)*BOT
221       13 CONTINUE
223          MUL=BOT/TOP
225          SUM=0.0
226          DO 14 N=1,L1
227          AN=N
230          IF(AN-2.)85,86,87
233       85 TOD=1.
235          GO TO 88
235       86 TOD=AL1
237          GO TO 88
237       87 CONTINUE
237          TOD=1.
241          ICH=L1-(N-2)
244          DO 15 J=ICH,L1
245          AJ=J
246          TOD=AJ*TOD
```

```
   15 CONTINUE
   88 CONTINUE
      BOD=1.
      JA=L1+N
      DO 16 J=L,JA
      AJ=J
      BOD=BOD*(AJ+BET)
   16 CONTINUE
      CO=TOD/BOD
      SUM=SUM+CO*A(N)
   14 CONTINUE
      A(L)=MUL*(DEL*F-SUM)
   11 CONTINUE
      CALL JACSER(DEL,A,BET)
      CALL NAMPLT
      CALL QIKSET(6.0,0.0,0.0,6.0,0.0,0.0)
      CALL QIKSAX(3,3)
      CALL QIKPLT(TT,BK,101)
      CALL ENDPLT
   10 CONTINUE
  999 CONTINUE
      RETURN
      END
```

```
      SUBROUTINE JACSER(D,C,B)
      DIMENSION C(50),SF(50),P(50)
      DIMENSION BK(101),TT(101)
      COMMON/2/TI,TF,DT,MN,BK,TT
      TT(1)=0.0
      BK(1)=0.0
      LM=1
      T=TI
   12 T=T+DT
      X=2.*EXP(-D*T)-1.
      CALL JACOBI(MN,X,B,P)
      SF(1)=C(1)*P(1)
      DO 10 L=2,MN
      L1=L-1
      AL=L
      SF(L)=SF(L1)+C(L)*P(L)
   10 CONTINUE
      PRINT 97,T,X
   97 FORMAT(/////5X,*  T =*F6.3,*  X =*F10.5)
      PRINT 96
   96 FORMAT(///5X,* I    C(I)     *,5X,* N    F(T)     *)
      DO 11 I=1,6
      PRINT 95,I,C(I),I,SF(I)
   95 FORMAT(5X,I2,F10.2,5X,I2,F10.5)
   11 CONTINUE
      LM=LM+1
      BK(LM)=SF(5)
      TT(LM)=T
      IF(T.LE.TF) GO TO 12
      RETURN
      END
```

```
      SUBROUTINE JACOBI(N,X,B,PB)
C     THIS PROGRAM CALCULATES JACOBI POLYNOMIALS OF ORDER
C     K-1 WITH ARG X AND PARAMETER B GT -1
      DIMENSION PB(N)
      AN=N
      IF(AN-2.)1,2,3
    1 PB(1)=1.
      RETURN
    2 PB(1)=1.
      PB(2)=X-B*(1.-X)/2.
      RETURN
    3 BSQ=B*B
      BONE=B+1.
      PB(1)=1.
      PB(2)=X-B*(1.-X)/2.
      DO 4 K=3,N
      AK=K
```

```
      AK1=AK-1.
      AK2=AK-2.
      K1=K-1
      K2=K-2
      C01=((2.*AK1)+B)*X
      C01=((2.*AK2)+B)*C01
      C01=((2.*AK2)+BONE)*(C01-BSQ)
      C02=2.*AK2*(AK2+B)*((2.*AK1)+B)
      C0=2.*AK1*(AK1+B)*((2.*AK2)+B)
    4 PB(K)=(C01*PB(K1)-C02*PB(K2))/C0
      RETURN
      END


      SUBROUTINE SPLINE(X,Y,M,C,XINT,YINT)
      DIMENSION X(50),Y(50),C(4,50)
      IF(XINT-X(1))1,10,11
   10 YINT=Y(1)
      RETURN
   11 CONTINUE
      IF(X(M)-XINT)1,12,13
   12 YINT=Y(M)
      RETURN
   13 CONTINUE
      K=M/2
      N=M
    2 CONTINUE
      IF(X(K)-XINT)3,14,5
   14 YINT=Y(K)
      RETURN
    3 CONTINUE
      IF(XINT-X(K+1))4,15,7
   15 YINT=Y(K+1)
      RETURN
    4 CONTINUE
      YINT=(X(K+1)-XINT)*(C(1,K)*(X(K+1)-XINT)**2+C(3,K))
      YINT=YINT+(XINT-X(K))*(C(2,K)*(XINT-X(K))**2+C(4,K))
      RETURN
    5 CONTINUE
      IF(X(K-1)-XINT)6,16,17
    6 K=K-1
      GO TO 4
   16 YINT=Y(K-1)
      RETURN
   17 N=K
      K=K/2
      GO TO 2
    7 LL=K
      K=(N+K)/2
    8 CONTINUE
      IF(X(K)-XINT)3,14,18
   18 CONTINUE
      IF(X(K-1)-XINT)6,16,19
   19 N=K
      K=(LL+K)/2
      GO TO 8
    1 PRINT 101
  101 FORMAT(* OUT OF RANGE FOR INTERPOLATION  *)
      STOP
      END


      SUBROUTINE SPLICE(X,Y,M,C)
      DIMENSION X(50),Y(50),D(50),P(50),E(50),C(4,50)
      DIMENSION A(50,3),B(50),Z(50)
      MM=M-1
      DO 2 K=1,MM
      D(K)=X(K+1)-X(K)
      P(K)=D(K)/6.
    2 E(K)=(Y(K+1)-Y(K))/D(K)
      DO 3 K=2,MM
    3 B(K)=E(K)-E(K-1)
      A(1,2)=-1.-D(1)/D(2)
      A(1,3)=D(1)/D(2)
      A(2,3)=P(2)-P(1)*A(1,3)
```

```
      A(2,2)=2.*(P(1)+P(2))-P(1)*A(1,2)
      A(2,3)=A(2,3)/A(2,2)
      B(2)=B(2)/A(2,2)
      DO 4 K=3,MM
      A(K,2)=2.*(P(K-1)+P(K))-P(K-1)*A(K-1,3)
      B(K)=B(K)-P(K-1)*B(K-1)
      A(K,3)=P(K)/A(K,2)
    4 B(K)=B(K)/A(K,2)
      Q=D(M-2)/D(M-1)
      A(M,1)=1.+Q+A(M-2,3)
      A(M,2)=-Q-A(M,1)*A(M-1,3)
      B(M)=B(M-2)-A(M,1)*B(M-1)
      Z(M)=B(M)/A(M,2)
      MN=M-2
      DO 6 I=1,MN
      K=M-I
    6 Z(K)=B(K)-A(K,3)*Z(K+1)
      Z(1)=-A(1,2)*Z(2)-A(1,3)*Z(3)
      DO 7 K=1,MM
      Q=1./(6.*D(K))
      C(1,K)=Z(K)*Q
      C(2,K)=Z(K+1)*Q
      C(3,K)=Y(K)/D(K)-Z(K)*P(K)
    7 C(4,K)=Y(K+1)/D(K)-Z(K+1)*P(K)
      RETURN
      END
```

INTERIM REPORT DISTRIBUTION LIST

NSG 3179

"OFF-AXIS IMPACT OF UNIDIRECTIONAL COMPOSITES WITH CRACKS: DYNAMIC STRESS INTENSIFICATION"

Advanced Research Projects Agency
Washington DC 20525
Attn: Library

Advanced Technology Center, Inc.
LTV Aerospace Corporation
P.O. Box 6144
Dallas, TX 75222
Attn: D. H. Petersen
W. J. Renton

Air Force Flight Dynamics Laboratory
Wright-Patterson Air Force Base, OH 45433
Attn: L. J. Obery (TBP)
G. P. Sendeckyj (FBC)
R. S. Sandhu

Air Force Materials Laboratory
Wright-Patterson Air Force Base, OH 45433
Attn: H. S. Schwartz (LN)
T. J. Reinhart (MBC)
G. P. Peterson (LC)
E. J. Morrisey (LAE)
S. W. Tsai (MBM)
N. J. Pagano
J. M. Whitney (MBM)

Air Force Office of Scientific Research
Washington DC 20333
Attn: J. F. Masi (SREP)

Air Force Office of Scientific Research
1400 Wilson Blvd.
Arlington, VA 22209

AFOSR/NA
Bolling AFB, DC 20332
Attn: W. J. Walker

Air Force Rocket Propulsion Laboratory
Edwards, CA 93523
Attn: Library

Babcock & Wilcox Company
Advanced Composites Department
P.O. Box 419
Alliance, Ohio 44601
Attn: P. M. Leopold

Bell Helicopter Company
P.O. Box 482
Ft. Worth, TX 76101
Attn: H. Zinberg

The Boeing Company
P. O. Box 3999
Seattle, WA 98124
Attn: J. T. Hoggatt, MS. 88-33
T. R. Porter

The Boeing Company
Vertol Division
Morton, PA 19070
Attn: R. A. Pinckney
E. C. Durchlaub

Battelle Memorial Institute
Columbus Laboratories
505 King Avenue
Columbus, OH 43201
Attn: E. F. Rybicki
L. E. Hulbert

Brunswick Corporation
Defense Products Division
P. O. Box 4594
43000 Industrial Avenue
Lincoln, NE 68504
Attn: R. Morse

Celanese Research Company
86 Morris Ave.
Summit, NJ 07901
Attn: H. S. Kliger

Chemical Propulsion Information Agency
Applied Physics Laboratory
8621 Georgia Avenue
Silver Spring, MD 20910
Attn: Library

Commander
Natick Laboratories
U. S. Army
Natick, MA 01762
Attn: Library

Commander
Naval Air Systems Command
U. S. Navy Department
Washington DC 20360
Attn: M. Stander, AIR-43032D

Commander
Naval Ordnance Systems Command
U.S. Navy Department
Washington DC 20360
Attn: B. Drimmer, ORD-033
M. Kinna, ORD-033A

Cornell University
Dept. Theoretical & Applied Mech.
Thurston Hall
Ithaca, NY 14853
Attn: S. L. Phoenix

Defense Metals Information Center
Battelle Memorial Institute
Columbus Laboratories
505 King Avenue
Columbus, OH 43201

Department of the Army
U.S. Army Material Command
Washington DC 20315
Attn: AMCRD-RC

Department of the Army
U.S. Army Aviation Materials Laboratory
Ft. Eustis, VA 23604
Attn: I. E. Figge, Sr.
Library

Department of the Army
U.S. Army Aviation Systems Command
P.O. Box 209
St. Louis, MO 63166
Attn: R. Vollmer, AMSAV-A-UE

Department of the Army
Plastics Technical Evaluation Center
Picatinny Arsenal
Dover, NJ 07801
Attn: H. E. Pebly, Jr.

Department of the Army
Watervliet Arsenal
Watervliet, NY 12189
Attn: G. D'Andrea

Department of the Army
Watertown Arsenal
Watertown, MA 02172
Attn: A. Thomas

Department of the Army
Redstone Arsenal
Huntsville, AL 35809
Attn: R. J. Thompson, AMSMI-RSS

Department of the Navy
Naval Ordnance Laboratory
White Oak
Silver Spring, MD 20910
Attn: R. Simon

Department of the Navy
U.S. Naval Ship R&D Laboratory
Annapolis, MD 21402
Attn: C. Hersner, Code 2724

Director
Deep Submergence Systems Project
6900 Wisconsin Avenue
Washington DC 20015
Attn: H. Bernstein, DSSP-221

Director
Naval Research Laboratory
Washington DC 20390
Attn: Code 8430
I. Wolock, Code 8433

Drexel University
32nd and Chestnut Streets
Philadelphia, PA 19104
Attn: P. C. Chou

E. I. DuPont DeNemours & Co.
DuPont Experimental Station
Wilmington, DE 19898
Attn: C. H. Zweben

Fiber Science, Inc.
245 East 157 Street
Gardena, CA 90248
Attn: E. Dunahoo

General Dynamics
P.O. Box 748
Ft. Worth, TX 76100
Attn: M. E. Waddoups
Library

General Dynamics/Convair
P.O. Box 1128
San Diego, CA 92112
Attn: J. L. Christian

General Electric Co.
Evendale, OH 45215
Attn: C. Stotler
R. Ravenhall
R. Stabrylla

General Motors Corporation
Detroit Diesel-Allison Division
Indianapolis, IN 46244
Attn: M. Herman

Georgia Institute of Technology
School of Aerospace Engineering
Atlanta, GA 30332
Attn: L. W. Rehfield

Grumman Aerospace Corporation
Bethpage, Long Island, NY 11714
Attn: S. Dastin
J. B. Whiteside

Hamilton Standard Division
United Aircraft Corporation
Windsor Locks, CT 06096
Attn: W. A. Percival

Hercules, Inc.
Allegheny Ballistics Laboratory
P. O. Box 210
Cumberland, MD 21053
Attn: A. A. Vicario

Hughes Aircraft Company
Culver City, CA 90230
Attn: A. Knoell

Illinois Institute of Technology
10 West 32 Street
Chicago, IL 60616
Attn: L. J. Broutman

IIT Research Institute
10 West 35 Street
Chicago, IL 60616
Attn: I. M Daniel

Jet Propulsion Laboratory
4800 Oak Grove Drive
Pasadena, CA 91103
Attn: Library

Lawrence Livermore Laboratory
P.O. Box 808, L-421
Livermore, CA 94550
Attn: T. T. Chiao
E. M. Wu

Lehigh University
Institute of Fracture &
Solid Mechanics
Bethlehem, PA 18015
Attn: G. C. Sih

Lockheed-Georgia Co.
Advanced Composites Information Center
Dept. 72-14, Zone 402
Marietta, GA 30060
Attn: T. M. Hsu

Lockheed Missiles and Space Co.
P.O. Box 504
Sunnyvale, CA 94087
Attn: R. W. Fenn

Lockheed-California
Burbank, CA 91503
Attn: J. T. Ryder
K. N. Lauraitis
J. C. Ekvall

McDonnell Douglas Aircraft Corporation
P.O. Box 516
Lambert Field, MS 63166
Attn: J. C. Watson

McDonnell Douglas Aircraft Corporation
3855 Lakewood Blvd.
Long Beach, CA 90810
Attn: L. B. Greszczuk

Material Sciences Corporation
1777 Walton Road
Blue Bell, PA 19422
Attn: B. W. Rosen

Massachusetts Institute of Technology
Cambridge, MA 02139
Attn: F. J. McGarry
J. F. Mandell
J. W. Mar

NASA-Ames Research Center
Moffett Field, CA 94035
Attn: Library

NASA-Flight Research Center
P.O. Box 273
Edwards, CA 93523
Attn: Library

NASA-George C. Marshall Space Flight Center
Huntsville, AL 35812
Attn: C. E. Cataldo, S&E-ASTN-MX
Library

NASA-Goddard Space Flight Center
Greenbelt, MD 20771
Attn: Library

NASA-Langley Research Center
Hampton, VA 23365
Attn: E. E. Mathauser, MS 188a
R. A. Pride, MS 188a
M. C. Card
J. R. Davidson

NASA-Lewis Research Center
21000 Brookpark Road
Cleveland, Ohio 44135
Attn: Administration & Technical Service Section
Tech. Report Control, MS. 5-5
Tech. Utilization, MS 3-19
AFSC Liaison, MS. 501-3
Rel. and Quality Assur., MS 500-211
C. P. Blankenship, MS 105-1
R. F. Lark, MS 49-3
J. C. Freche, MS 49-1
R. H. Johns, MS 49-3
C. C. Chamis, MS 49-3 (17 copies)
T. T. Serafini, MS 49-1
Library, MS 60-3 (2 copies)

NASA-Lyndon B. Johnson Space Center
Houston, TX 77001
Attn: S. Glorioso, SMD-ES52
Library

NASA Scientific and Tech. Information Facility
P.O. Box 8757
Balt/Wash International Airport, MD 21240
Attn: Acquisitions Branch (10 copies)

National Aeronautics & SpaceAdministration
Office of Advanced Research & Technology
Washington DC 20546
Attn: M. J. Salkind, Code RWS
D. P. Williams, Code RWS

National Aeronautics & Space Administration
Office of Technology Utilization
Washington DC 20546

National Bureau of Standards
Eng. Mech. Section
Washington DC 20234
Attn: R. Mitchell

National Technology Information Service
Springfield, VA 22151 (6 copies)

National Science Foundation
Engineering Division
1800 G. Street, NW
Washington DC 20540
Attn: Library

Northrop Corporation Aircraft Group
3901 West Broadway
Hawthorne, CA 90250
Attn: R. M. Verette
G. C. Grimes

Pratt & Whitney Aircraft
East Hartford, CT 06108
Attn: A. J. Dennis

Rockwell International
Los Angeles Division
International Airport
Los Angles, CA 90009
Attn: L. M. Lackman
D. Y. Konishi

Sikorsky Aircraft Division
United Aircraft Corporation
Stratford, CT 06602
Attn: Library

Southern Methodist University
Dallas, TX 75275
Attn: R. M. Jones

Southwest Research Institute
8500 Culebra Road
San Antonio, TX 78284
Attn: P. H. Francis

Space & Missile Systems Organization
Air Force Unit Post Office
Los Angeles, CA 90045
Attn: Technical Data Center

Structural Composites Industries, Inc.
6344 N. Irwindale Avenue
Azusa, CA 91702
Attn: R. Gordon

Texas A&M
Mechanics & Materials Research Center
College Station, TX 77843
Attn: R. A. Schapery

TRW, Inc.
23555 Euclid Avenue
Cleveland, OH 44117
Attn: W. E. Winters

Union Carbide Corporation
P. O. Box 6116
Cleveland, OH 44101
Attn: J. C. Bowman

United Technologies Research Center
East Hartford, CT 06108
Attn: R. C. Novak

University of Dayton Research Institute
Dayton, OH 45409
Attn: R. W. Kim

University of Delaware
Mechanical & Aerospace Engineering
Newark, DE 19711
Attn: B. R. Pipes

University of Illinois
Department of Theoretical & Applied Mechanics
Urbana, IL 61801
Attn: S. S. Wang

University of Oklahoma
School of Aerospace Mechanical & Nuclear Engineering
Norman, OK 73069
Attn: C. W. Bert

University of Wyoming
College of Engineering
University Station Box 3295
Laramie, WY 82071
Attn: D. F. Adams

U. S. Army Materials & Mechanics Research Center
Watertown Arsenal
Watertown, MA 02172
Attn: E. M. Lenoe
D. W. Oplinger

V.P. I. and S. U.
Dept. of Eng. Mech.
Blacksburg, VA 24061
Attn: R. H. Heller
H. J. Brinson
C. T. Herakovich